

**The first exposure age for raised glaciomarine deltas:
Auburn Plains Delta, Southern Maine**

Denise Brushett
Department of Earth Sciences
Dalhousie University

Advisor
John Gosse
Department of Earth Sciences
Dalhousie University

Submitted in partial fulfillment of the requirements for the Degree of Honours Bachelor
of Science Earth Sciences,
Dalhousie University, Halifax, Nova Scotia



Dalhousie University

Department of Earth Sciences

Halifax, Nova Scotia

Canada B3H 3J5

(902) 494-2358

FAX (902) 494-6889

DATE: April 29 / 2005

AUTHOR: Denise Michelle Brushett

TITLE: The First Exposure Age For Raised Glaciomarine Deltas:

Auburn Plains Delta, Southern Maine

Degree: B. Sc. Convocation: May 2005 Year: 2005

Permission is herewith granted to Dalhousie University to circulate and to have copied for non-commercial purposes, at its discretion, the above title upon the request of individuals or institutions.

THE AUTHOR RESERVES OTHER PUBLICATION RIGHTS, AND NEITHER THE THESIS NOR EXTENSIVE EXTRACTS FROM IT MAY BE PRINTED OR OTHERWISE REPRODUCED WITHOUT THE AUTHOR'S WRITTEN PERMISSION.

THE AUTHOR ATTESTS THAT PERMISSION HAS BEEN OBTAINED FOR THE USE OF ANY COPYRIGHTED MATERIAL APPEARING IN THIS THESIS (OTHER THAN BRIEF EXCERPTS REQUIRING ONLY PROPER ACKNOWLEDGEMENT IN SCHOLARLY WRITING) AND THAT ALL SUCH USE IS CLEARLY ACKNOWLEDGED.

Abstract

Late Pleistocene ice contact glaciomarine deltas indicate the deglacial sea-level to which the deltas were graded at successive ice positions and record the inland limit of marine submergence. Precise age determinations for topset-foreset contacts provide a valuable chronology of the timing and rate of deglaciation as well as the duration of marine submergence and its relationship to postglacial uplift. The present study aims to test the reliability of using terrestrial in situ-produced cosmogenic nuclide (TCN) exposure dating on raised glaciomarine deltas where a radiocarbon based chronology exists for comparison. The Auburn Plains glaciomarine delta in southern Maine was exposure dated using cosmogenic ^{10}Be measured in five sand samples collected in a vertical profile (94 to 265 cm depth) beneath the sediment mixing zone. The samples contained 1.46×10^4 atom g^{-1} of inherited ^{10}Be produced in the quartz prior to delta deposition. After minor (<1%) adjustments for snow and vegetation cover, and change in the integrated production rate due to isostatic uplift (1.6%), the apparent exposure age (ignoring erosion) of the Auburn Plains delta is 11.0 ± 0.9 ka (2σ). A sensitivity analysis was performed to evaluate the influence on the apparent exposure age of uncertainties in bulk density and surface erosion. While the apparent exposure age is a minimum age due to a potentially high sensitivity to erosion which would reduce the exposure age, the precision of the measurement is comparable to radiocarbon dating. When compared to published maximum limiting radiocarbon ages for the Auburn Plains delta (mean = 14.7 ka), an average constant erosion rate of 0.035 mm yr^{-1} (or 52 cm of sediment removed) would be required to explain the disparity.

Table of Contents

Abstract	2
Table of Contents	3
List of Figures	4
List of Tables	5
Chapter 1: Introduction	7
Chapter 2: Geological background	14
2.1 Physiography of southern and coastal Maine.....	14
2.2 Glaciomarine deposits	15
2.3 Existing chronology for southern and coastal Maine	21
2.4 Glacial history of southern and coastal Maine.....	25
2.5 TCN principles.....	28
Chapter 3: Methods	32
3.1 TCN dating of deltas.....	32
3.2 Site selection.....	35
3.3 Sample preparation and calculations.....	36
3.4 Age comparisons	40
Chapter 4: Results	42
4.1 ¹⁰ Be concentrations.....	42
4.2 Interpretation of concentrations as ages.....	46
4.3 Inheritance adjustments.....	46
4.4 Uncertainties.....	50
4.5 Adjustments for other factors.....	50
4.6 Sensitivity analysis.....	54
Chapter 5: Interpretations	57
5.1 Interpretation of the exposure age of Auburn Plains delta	57
5.2 Accuracy and comparison with pre-existing chronology.....	57
Chapter 6: Conclusions and Future work.....	61
References	63
Appendices:	
Appendix 1: Chemistry data.....	66
Appendix 2: AMS data	86
Appendix 3: Snow depth calculations	89

List of Figures

Figure 1.1: Surficial geology map of Maine.....	12
Figure 1.2: Digital elevation model of Maine.....	13
Figure 1.3: Digital elevation model of Maine showing the locations of the three glaciomarine ice-contact esker-fed deltas.....	13
Figure 2.1: Physiographic zones of Maine.....	15
Figure 2.2: Locations of surveyed glaciomarine deltas by Thompson et al. (1989) with respect to the marine limit.....	17
Figure 2.3: Characteristic features of Gilbert-type deltas.....	18
Figure 2.4: Deglacial chronology map of Maine showing deglaciation isochrones estimated from radiocarbon ages taken from marine and terrestrial samples.....	24
Figure 2.5: The sequence of deglaciation and deposition of surficial materials in Southern Maine between ~17.4 to 15.2 ka.....	26
Figure 2.6: The sequence of deglaciation and deposition of surficial materials in Southern Maine after 15.2 ka.....	27
Figure 2.7: Theoretical depth profile for a decrease in concentration of ^{10}Be (atom g^{-1}) with depth (cm) for Auburn Plains delta at an elevation of 113m....	31
Figure 3.1: TCN concentration history of a clast through its transport history.....	33
Figure 4.1: ^{10}Be concentrations for all samples from Auburn Plains delta.....	43
Figure 4.2: ^{10}Be concentrations for four samples from Auburn Plains delta, excluding outlier.....	43
Figure 4.3: ^{10}Be concentrations for four samples from Dayton delta.....	44
Figure 4.4: ^{10}Be concentrations for samples from Jailhouse delta.....	44
Figure 4.5: Inheritance-adjusted concentrations for Auburn Plains delta, excluding outlier.....	48
Figure 4.6: Exposure ages for Auburn Plains Delta.....	49
Figure 4.7: Effects of inheritance on exposure ages of Auburn Plains delta.....	49
Figure 4.8: Postglacial relative sea-level change curve at Barbados, which extends from the Last Glacial Maximum (LGM).....	52
Figure 4.9: The time integrated production rate for Auburn Plains delta over 15 ka where 0 yr is the present.....	52
Figure 4.10: Effects on TCN ages by snow cover of common densities and thicknesses.....	54
Figure 4.11: Effects of density on the exposure age of Auburn Plains delta.....	55
Figure 4.12: Effects of erosion on the exposure age of Auburn Plains delta.....	56

List of Tables

Table 3.1: Sample information for samples from Auburn Plains delta, Jailhouse delta and Dayton delta.....	40
Table 4.1: TCN concentrations, exposure ages, and inheritance calculated for samples from 3 deltas.....	45
Table 4.2: Time integrated production rate ($\text{atom g}^{-1} \text{yr}^{-1}$) for a rising surface that starts at sea-level.....	53
Table 5.1: Radiocarbon ages from Auburn Plains delta vicinity used to establish the deglaciation chronology of Maine.....	58
Table 5.2: Factors that may explain the difference between the ^{14}C and TCN ages.....	60

Acknowledgements

I extend my greatest thanks to my advisor, John Gosse who went above and beyond the expectations of any advisor by inspiring me think independently, to always question the data, and to have fun at the same time.

I would like to thank my parents and sisters for putting up with me throughout the year and my friends for their unending support this year especially Theo Popma, Sophie Baker, Jane Staiger, Victoria Burdett-Coutts, and Joyia Chakungal. Special thanks to Guang Yang for all her chemistry teaching and mothering throughout the year. I would like to thank Dr. Robert Finkel for running all my samples through AMS, and Dr. Woodrow Thompson for providing information on the surficial geology of Maine. I would also like to thank the following people for all their help and positive feedback: Dr. Ralph Stea, Dr. David Piper, Dr. Marcos Zentilli and Dr. Martin Gibling. Finally, I thank my fellow classmates for making this year so memorable.

Introduction

As the ice margin of the Late Wisconsinan Laurentide Ice Sheet (LIS) retreated from the continental shelf of Maine, there was widespread marine transgression and deposition of glaciomarine sediment across southern and coastal Maine (Thompson, 1982; Thompson et al., 1989). Glaciomarine muds and clays of the Presumpscot Formation and deltaic sediments conformably cover and interfinger with glacial deposits everywhere below the marine limit (Figure 1.1) (Thompson, 1982; Thompson and Borns, 1985b). Examination of this relationship between ice contact and glaciomarine deposits indicates that the sea was in contact with the retreating ice margin during much of the deglaciation (Thompson, 1989).

During and following deglaciation, isostatic adjustment accompanied a rising sea-level. Everywhere below the Late Pleistocene marine limit, the rate of sea-level rise exceeded the rate of isostatic uplift. At different times along the northern New England shore the rate of uplift eventually exceeded the rate of sea-level rise and caused emergence (Thompson et al., 1989; Koteff et al., 1993). Elevations of the contact between the topsets and foresets in raised glaciomarine deltas indicate the deglacial sea-level to which the deltas were graded at successive ice positions. Topset-foreset contacts are used to establish the inland limit of marine submergence (Koteff et al., 1993). It is important to precisely date these contacts because although the glacial geology of coastal Maine has been the subject of many investigations since the early 1800's, the timing and rate of deglaciation as well as the duration of marine submergence and its relationship to post-glacial uplift are still not well understood (Koteff et al., 1993; Dorion et al., 2001; Borns et al., 2004).

Dating the topset-foreset contacts and determining the relative sea-level history of Maine is difficult in part due to the lack of radiocarbon dateable material in glaciomarine deltas. Deltaic environments are unfavourable habitats for marine organisms because of rapid sedimentation rates and the influx of fresh water (Thompson, 1982). The existing chronology depends heavily on ^{14}C ages from marine shells (including *Portlandia arctica*, *Mya arenaria*, *Mya truncata*, *Mytilus edulis*, *Hiatella arctica*) found predominantly in the glaciomarine bottomset muds and clays that form the Presumpscot Formation and on the dating of kettle lake sediments (Thompson, 1982; Dorion et al., 2001; Borns et al., 2004). Few of these dates can be tied with reasonable assurance to positions along the retreating margin (Smith, 1985).

^{14}C ages from shells in the Presumpscot Formation provide an indirect (maximum or minimum bracketing) age on the paleo-sea-level depending on the stratigraphic relationship with the topset-foreset contact. Radiocarbon ages on basal kettle lake sediment in ice-contact deltas are useful because kettle lakes imply a close temporal and spatial relationship with the ice margin (Thompson et al., 1999; Dorion et al., 2001). Dates from kettle lakes may yield anomalously old ages from contamination by ^{14}C -dead organic materials that do not obtain their carbon directly from the atmosphere. For example, there are large ^{14}C errors from aquatic plant remain samples in New Hampshire that yielded ^{14}C ages that are 9 ky older than nonaquatic plants from the same beds (Ridge et al., 2001). In this case the lake ages will overestimate the true age of the topset-foreset contact. It is also possible that sedimentation may not have started immediately after the lake formation.

Most of these dates were obtained prior to the development of accelerator mass

spectrometry (AMS) ^{14}C analysis and improved laboratory techniques, which are now being used to obtain more reliable ^{14}C analyzes from small non-aquatic plant macrofossils (Ridge et al., 2001). ^{14}C dating of terrestrial plant macrofossils (used to calibrate the New England varve chronology) by Ridge et al. (2001) suggests that a combined reservoir and meltwater correction of 1.0 - 2.0 ka is necessary to make the atmospheric and uncorrected marine ^{14}C ages in southern Maine compatible (Ridge et al., 2001).

Terrestrial in situ produced cosmogenic nuclide (TCN) exposure dating provides a means to precisely date surface exposure durations. Prior to the 1980's difficulties in measuring low concentrations of cosmogenic nuclides produced at earth surfaces hindered cosmogenic nuclide applications. Measurements were facilitated by the development of AMS in the mid-1980's, which allowed isotopic ratios as low as 10^{-15} to be measured. Measurements of 10^4 atoms in a mole of mineral atoms are now routine (Gosse and Phillips, 2001). TCN dating is now being applied to a broad range of geological and geochronological problems on rock surfaces of different lithologies on all seven continents for time spans ranging from the Miocene (>10.4 Ma) to the late Holocene (<10 ka) (Gosse and Phillips, 2001).

Using TCN dating, deltaic sediments from the topset-foreset contact can be dated directly to provide a more precise indication for the timing of the ice margin retreat in the region. Furthermore, an exposure age on the topset-foreset contact can date the timing of relative sea-level change since deglaciation. The present study is only the second known study to attempt to date sediments from deltas. A previous attempt by Hilchey on Baffin Island (Hilchey, 2004) failed due to the retention of cosmogenic nuclides (inheritance)

from a previous period of exposure prior to delta deposition. Hilchey (2004) proposed that high inheritance occurred on Baffin Island as a result of cold-based (non-erosive) ice. Since there was little erosion, the sediment retained cosmogenic ^{10}Be from exposure prior to deposition of the deltas (Hilchey, 2004). Maine shows extensive evidence of warm-based (erosive) ice so that any previously accumulated isotope concentrations should be removed by glacial erosion.

The present study was conducted on three glaciomarine deltas in southern Maine (Figure 1.2, Figure 1.3) to test the reliability of using TCNs to date deltas and to also improve the existing geochronology of the LIS margin and relative sea-level history. The hypothesis, that *TCN dating can precisely date deltaic sediment* was evaluated by comparing exposure ages to the existing ^{14}C chronology for three late Pleistocene glaciomarine deltas near the marine limit in southern Maine.

The morphology and stratigraphy of raised glaciomarine deltas in southern Maine commonly suggest that they were deposited adjacent to the ice margin (Thompson et al., 1989). Their elevation and distribution have been used to determine the isostatic uplift that occurred during and after deglaciation (Thompson, 1982; Thompson et al., 1989; Koteff et al., 1993). Recent attempts to compare the dynamics of the LIS with the paleoceanography of the Gulf of Maine have produced more radiocarbon dates from ice proximal deposits (Dorion et al., 2001; Borns et al. 2004) and the formulation of an atmospheric ^{14}C chronology (Ridge et al., 2001) that can be compared to the obtained cosmogenic exposure ages. Comparisons between the existing chronology and the exposure ages will determine whether TCN dating can be used to date raised deltas.

Three raised glaciomarine deltas in southern Maine were selected to test the

application of TCN dating of Pleistocene deltas (Figure 1.2, Figure 1.3). The three deltas are Auburn Plains Delta, Dayton delta, and Jailhouse delta. These deltas were selected because they were previously mapped and included in regional studies of delta elevations and post glacial isostatic uplift (Thompson and Borns, 1985b; Thompson et al., 1989; Koteff et al., 1993). These deltas also have well-studied stratigraphy (Thompson et al., 1989). The deltas are close to the marine limit where reworking of topset sediments by wave action and shielding from cosmic rays due to submergence are minimal. The deltas show little evidence of erosion or disturbance. They were sampled along pit boundaries that had their surfaces marked by stone fences indicating that property lines have remained undisturbed since they were emplaced. The presence of sedimentary structures indicated that that the topset-foreset contacts were still intact.

This thesis will further explain the selection of these deltas, the sampling strategy and TCN approach, and justify my conclusion that TCN exposure dating can successfully date raised deltaic sediments.

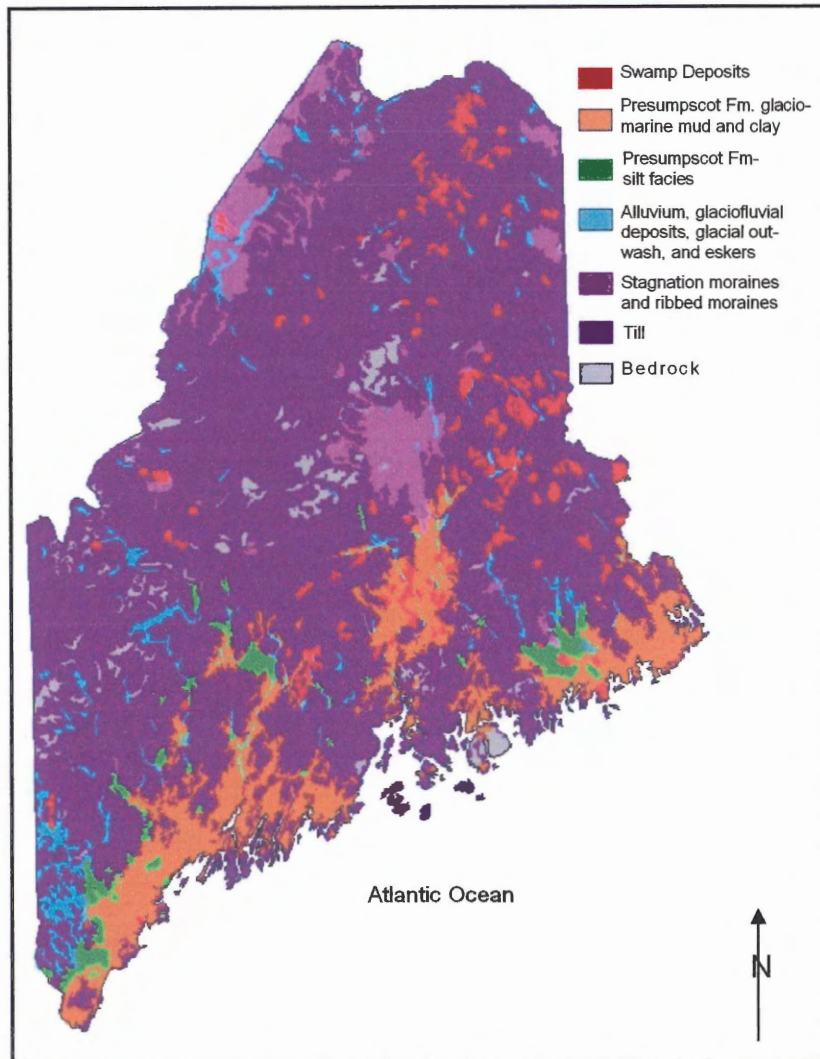


Figure 1.1 Surficial geologic map of Maine showing the relationship between the glaciomarine muds and clays of the Presumpscot Formation (orange) and glaciofluvial deposits (blue) that include deltas, glacial outwash deposits and eskers (modified from Maine Geological Survey).

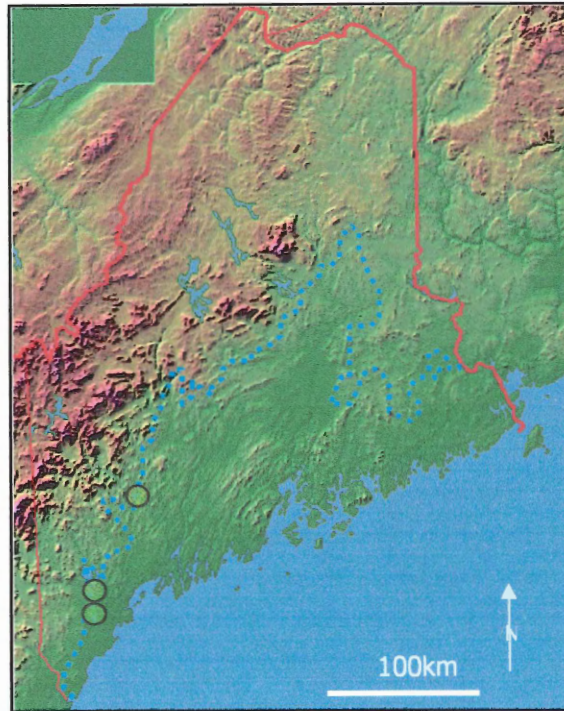


Figure 1.2 Digital elevation model of Maine showing the locations of the three glaciomarine ice-contact esker-fed deltas. Dotted line represents extent of maximum marine submergence. Elevation decreases from red to green. Modified from www.vitalsearch-ca.com/gen/me/me_.htm.

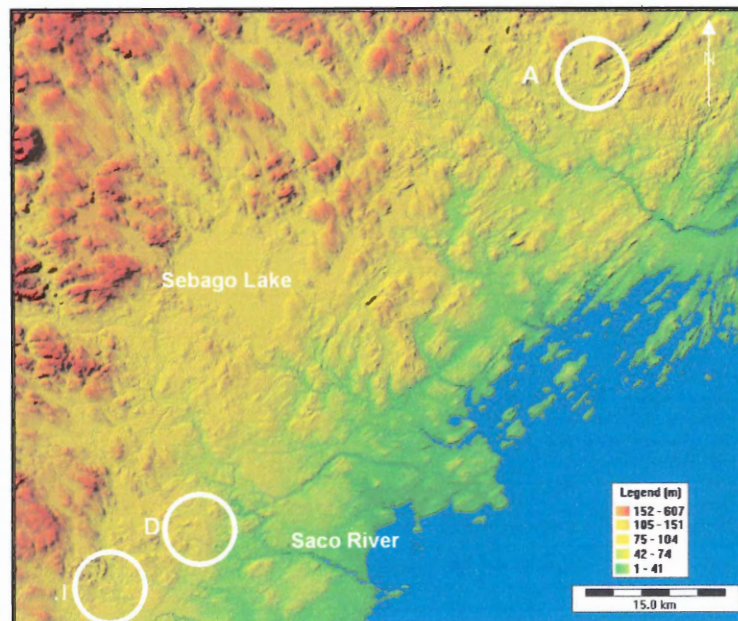


Figure 1.3 Digital elevation model (90m shuttle radar topographic mission data) of southern Maine showing the locations of the studied deltas. Auburn Plains delta (A) is 44.17°N , 70.24°W at 113 m elevation. Dayton delta (D) is 43.54°N , 70.6°W at 91 m elevation. Jailhouse delta (J) is 43.46°N , 70.72°W at 84 m elevation. Elevation decreases from red to green.

2 Background

2.1 Physiography of southern and coastal Maine

Southern and coastal Maine can be divided into three physiographic sections: White Mountains, New England Upland, and the Seaboard Lowland, as shown in Figure 2.1 (Smith, 1985). The Seaboard Lowlands are low relief surfaces with elevations that are typically below 90 m and are generally coincident with the area of marine submergence (Smith, 1985). Both the uplands and lowlands are underlain by a variety of Paleozoic metasedimentary rocks that have been intruded by Late Paleozoic granitic and gabbroic plutons that dip steeply and strike in a general northeast-southwest direction (Smith, 1985; Dorion et al., 2001).

During the Late Wisconsinan glaciation, ice advance was from the north and northwest (Smith, 1985). Glacial erosion produced northwest-southeast lineations superimposed on the northeast-southwest structural grain. Additional evidence for advance direction is found in valleys that parallel the direction of ice movement and streamlined erosional landforms. Glacial deposition preferentially infilled valleys resulting in reduced preglacial relief (Smith, 1985).

Topography is important in the formation of ice marginal deposits. Kettles occur where ice blocks were stranded in the lee of ridges. In southern Maine, bedrock ridges (relief > 100m) trend parallel to the general orientation of the retreating margin of the ice sheet. When these ridges temporarily anchored the ice margin, they enabled the deposition of ice-contact “leeside” glaciomarine deltas (Thompson et al., 1989).

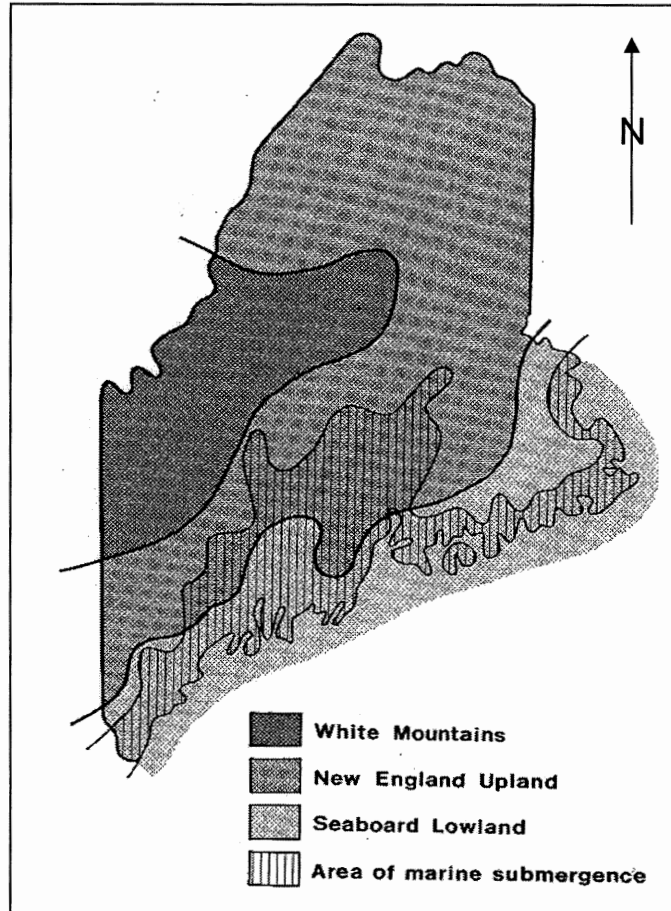


Figure 2.1. Physiographic zones of Maine. The area of late-glacial marine submergence is also shown (striped) (from Smith, 1985).

2.2 Glaciomarine deposits

2.2.1 Introduction

Maine experienced multiple ice advances during the Pleistocene Epoch, yet evidence of only the last glaciation is preserved on land (Hunter, 1990). The sequence of the deglaciation of Maine is most clearly defined across southern and coastal Maine where the glacial history has been reconstructed from numerous end moraines, deltas, and submarine fans that were deposited during an accompanying marine transgression of the coastal lowland that accompanied ice retreat. Marine transgression of lowland areas extended up to 175 km inland as the result of a time lag between ice retreat and isostatic

crustal uplift. The marine limit is defined as the maximum height, above present sea-level, where evidence of submergence by the sea is found in regions that are undergoing postglacial isostatic rebound (Peltier, 1998). A less detailed pattern of deglaciation is observed in Central Maine, inland from the marine limit, where reconstructions are built from features including striation patterns, melt water channels, scattered moraines and water-laid deposits that constrain the trend of the ice margin. In contrast to the coastal region, recession of the ice sheet across central and northern Maine is documented by extensive esker systems and few end moraines (Borns et al., 2004).

2.2.2 Glaciomarine Deltas

Over 100 glaciomarine deltas have been identified in Maine and there are likely more if you consider the numerous poorly exposed sand and gravel deposits (of uncertain origin) that occur near the inland marine limit. In one study on the glaciomarine deltas of Maine, Thompson et al.(1989) found that many of the deltas were clustered near the marine limit in eastern and south-western Maine (Figure 2.2). Other regions, such as central Maine show few deltas despite marine submergence of these regions. One proposed explanation is that ice retreat in central Maine occurred too rapidly for the deltas to build up. The southern Maine deltas are much larger than those in other regions in Maine. The presence of the larger size and number of deltas in these regions may be due to slower glacial retreat and stillstands as the ice margin became grounded in shallower water near the marine limit. Another important factor contributing to the size of these deltas is the large amounts of sand and gravel that originated from the glacial erosion of granitic plutons that occur either under the deltaic complexes or northwest of

them (Thompson et al, 1989).

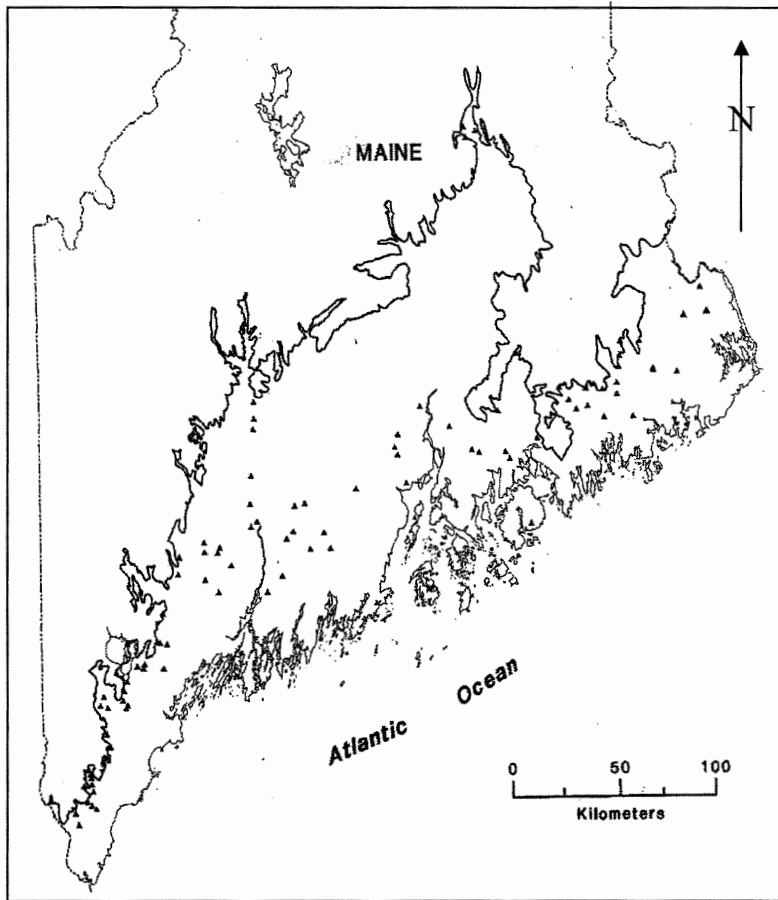


Figure 2.2 Locations of surveyed glaciomarine deltas by Thompson et al. (1989) with respect to the marine limit in Maine (from Thompson et al., 1989).

Measurements of maximum water depth in which the Maine deltas were deposited indicate that the deltas were deposited in shallow water. This data led Thompson et al. (1989) to conclude that the deltas formed next to the grounded margin of a tidewater glacier. Many of the deltas exhibit evidence of glaciotectonism (folding, reverse faulting, and normal faults indicating collapse after melting. Additionally, the ubiquitous presence of kettles and dropstones in the deltas support their glacial affinity. Stratified end moraines and submarine fans were also deposited near the grounding line

of the ice sheet (Thompson et al., 1989).

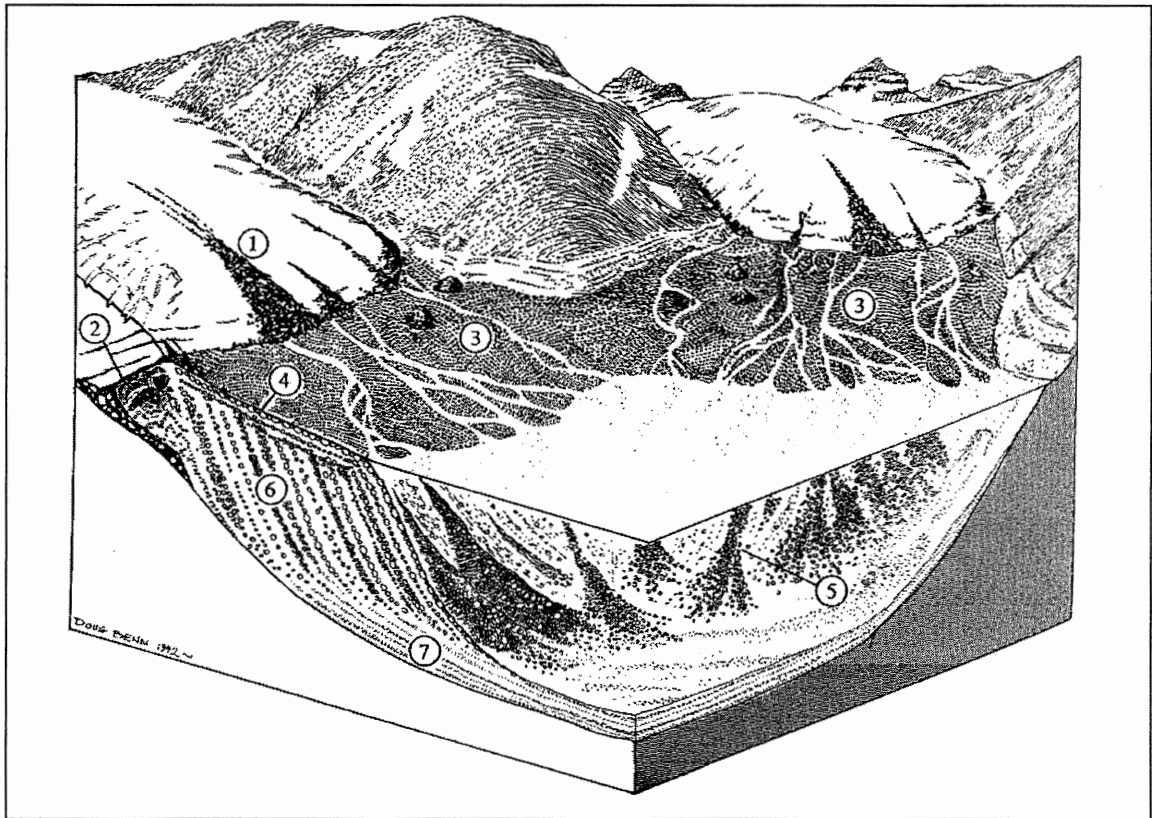


Figure 2.3 Characteristic features of Gilbert-type deltas. Supraglacial (1), englacial and subglacial (2) streams directly feed ice-contact deltas. The ice edge and delta front (5) are separated by a relatively short sandur surface (3). Gilbert type deltas are characterized by cross-bedded fluvial pebbly gravel topset beds (4), steeply dipping subaqueous sandy foreset beds (6), and silty bottomsets (7) (from Benn and Evans, 1998).

The majority of large raised Pleistocene deltas in Maine are Gilbert type deltas that formed from the discharge of sediment into the sea where the large sediment supply allowed deposits to build up to the sea surface (Figure 2.3). This permitted the formation of deltas with cross-bedded fluvial topset beds overlying steeply dipping foreset beds that were deposited on the prograding delta front. The relatively flat topset beds consist mostly of poorly sorted pebbly sand to cobbly gravel that was carried by high energy meltwater streams and deposited in distributaries that crossed the delta plain resulting in a seaward thinning wedge. The topset surfaces are marked by kettles and channels that are

graded to the contemporary sea-level. Kettles formed where sediment was deposited over blocks of stagnant ice that subsequently melted. Some of these surfaces were subsequently modified by marine erosion and postglacial stream terracing (Thompson et al., 1989).

The foreset beds built up in sequences up to 23 m thick as finer sand and gravel was carried past the distributary mouths and moved down the face of the delta front by avalanching grain flows and turbidity flows. The foreset beds are typically well stratified except in the proximal areas of deltas where coarse gravel was deposited by melt water streams at the ice margin. Foresets may show several deformation structures that result from rapid sedimentation and overloading or oversteepening of the foreset slope. These deformation structures include a variety of slump structures that range from slight Bennding and overturning of the foresets to complex folding and faulting where foreset beds have slid down the delta front (Thompson et al., 1989).

Topset-foreset contacts are important sea-level indicators that provide a minimum measure of the position of sea-level to which the delta was graded (Thompson et al., 1989). Deltas may lack well-preserved topset beds because they may have been replaced by a recessional facies deposited by wave reworking during transgression and regression (Thompson et al., 1989). It is necessary to ascertain whether the deltas do in fact have intact topset-foreset contacts that can be used as paleo-sea-level indicators (Gosse, 1994). Deltas near the marine limit have the lowest probability of containing a recessional facies.

The bottomsets are fine grained sub-horizontal silty sea floor deposits that accumulated in front of the deltas and are buried by overlying foresets as the deltas

prograded. Although the bottomsets are concealed by the overlying foresets that continued to build as the deltas prograded, they are thought to extend seaward from the delta fronts. In Maine, the marine Presumpscot Formation clays and silts cover the bottomsets and are commonly found either intertonguing or overlying foreset beds (Thompson et al., 1989).

2.2.3 Other Glacial Deposits

The deltas in the present study are all esker-fed ice contact deltas. Eskers mark the path of channels that carried sediment to the proximal parts of the deltas. Most of the eskers are De Geer type eskers that were deposited in successive segments that terminate at deltas or submarine fans (Thompson, 1982).

The majority of end moraines in coastal Maine are located below the marine limit. Field evidence suggests that they were deposited along the grounded tidewater glacial margin during brief still stands or minor readvances (Borns et al., 2004). They predominantly consist of stratified glacially-deposited sand and gravel that would have required high current velocities to transport them. Such currents emerged from the ice under hydrostatic pressure. Deposition then occurred along the grounding line where meltwater currents slackened as they entered the sea (Thompson, 1982). The orientation of end moraines and ice flow features indicates the northeast trend of the ice front and incremental northwest retreat pattern of the LIS in southern Maine (Borns et al., 2004).

Ice contact submarine fans which lack topsets are common within the moraine complexes and elsewhere below the marine limit. Some of them built up to the ocean surface and evolved into deltas. Like moraines and ice contact deltas, the fans record the

ice margin position and are an important source of aggregate (Thompson et al., 1989; Borns et al., 2004).

Above the marine limit, there are fewer end moraines, deltas or fans that can be used to reconstruct the deglacial history. A different mapping technique, the morphosequence mapping technique, developed by Koteff and Pessl (1981), can be applied in these regions and used to distinguish between ice contact heads of melt water deposits. Morphosequences are groups of associated water-lain deposits (such as glacio-lacustrine deltas and outwash) that were deposited in sequences such that more collapsed forms from the melting of ice are found at the head or upstream parts of outwash and progressively less collapsed forms occur downstream. Each morphosequence is controlled by the retreating ice and graded to a particular base level. For example, a morphosequence with a delta and associated outwash graded to the surface of a temporary glacial lake may have a moraine at the head of the valley, marking the location of the glacier that formed the dammed lake (Koteff and Pessl, 1981; Borns et al., 2004).

2.3 Existing Chronology for southern and coastal Maine

All radiocarbon dates reported have been calibrated using Calib 5.0.1. and are presented as years before present with 2σ uncertainty (Stuiver and Reimer, 2005).

The existing chronology of glacial recession has been constructed from radiocarbon ages from both marine and terrestrial ice proximal environments. Earlier studies by Stuiver and Borns (1975) and Smith (1985) attempted to determine the chronology of ice retreat of coastal Maine that formed the groundwork for further chronological investigations. While both of their studies were hindered by a lack of

reliable radiocarbon ages, they concluded that deglaciation of the coastal lowlands of Maine took place between $\sim 15.6 \pm 0.3$ ka and 14.8 ± 0.3 ka. Since that time, numerous studies including recent studies by Dorion et al. (2001), Ridge et al. (2001), and Borns et al. (2004) have improved the chronology of glacial recession.

Several factors still hinder the deglaciation chronology of southern Maine. Few pits or exposures contain in situ ice proximal fauna that are suitable for achieving closely limiting ages. Fossils are uncommon in glaciomarine deltas because the delta fronts formed unfavourable environments for life because of rapid sedimentation rates and the influx of fresh water (Thompson, 1982). Fossils are also rare in end moraines and only occur in the distal parts of moraines where they are interbedded with the fossiliferous Presumpscot Formation. Often fossils in the surface exposures of the Presumpscot Formation represent a regressive marine fauna that is somewhat younger than the time of deglaciation. Because it is rare to have fossils in the inter-bedded marine sediments, and because exposure of these sediments is typically limited to gravel pits and road cuts, it is usually not possible to directly date the landforms with ^{14}C . Instead, it is only possible to date the first organic material to accumulate above these landforms. However, these ages provide only minimum limiting ages for deposition and time of deglaciation. Above the marine limit, ages are determined from organic material from sediments in ponds and lakes that only provide minimum limiting ages of ice retreat (Borns et al., 2004).

Ridge et al. (2001) used terrestrial plant macrofossils, varve chronologies, and paleomagnetism from glacial lakes to formulate the first atmospheric ^{14}C chronology for the deglaciation of New Hampshire and Maine. The ^{14}C chronology is ~ 1.0 to 1.5 ky younger, on average, than uncorrected ^{14}C ages from marine fossils and lacustrine bulk

sediment samples that have previously been used to determine deglaciation chronologies and rates of isostatic uplift. Ridge et al. (2001) suggest that marine ^{14}C ages are anomalous due to a marine reservoir effect and the influences of glacial meltwater in the Gulf of Maine from the Late Wisconsinan glaciomarine environment. More recent work by Ridge suggest that a reservoir correction of -600 to -1300 years should be added to the marine radiocarbon ages in south-western Maine and -800 to -1000 years for most cases (J. Ridge, per. comm., in Born et al., 2004). This work is included in a recent review of the history of deglaciation of Maine, by Borns et al. (2004). This compilation adds significantly more detail to the history of deglaciation of Maine by building a database of previously obtained radiocarbon ages as well as new ages from terrestrial and marine environments that include marine shells and seaweed, pond and lake sediments, as well as plant and insect fragments. Figure 2.4 shows the map of deglaciation chronology with the sites and ages that have been used to constrain the timing of deglaciation. Time lines show generalized positions of the ice margin. A reservoir correction of only -600 years was added to marine ages, so it is still possible that these ages are still overestimated. Nevertheless, this is the state of the art of deglacial chronology for Maine, and forms the basis of the dates which I will use to test TCN dating of deltas.

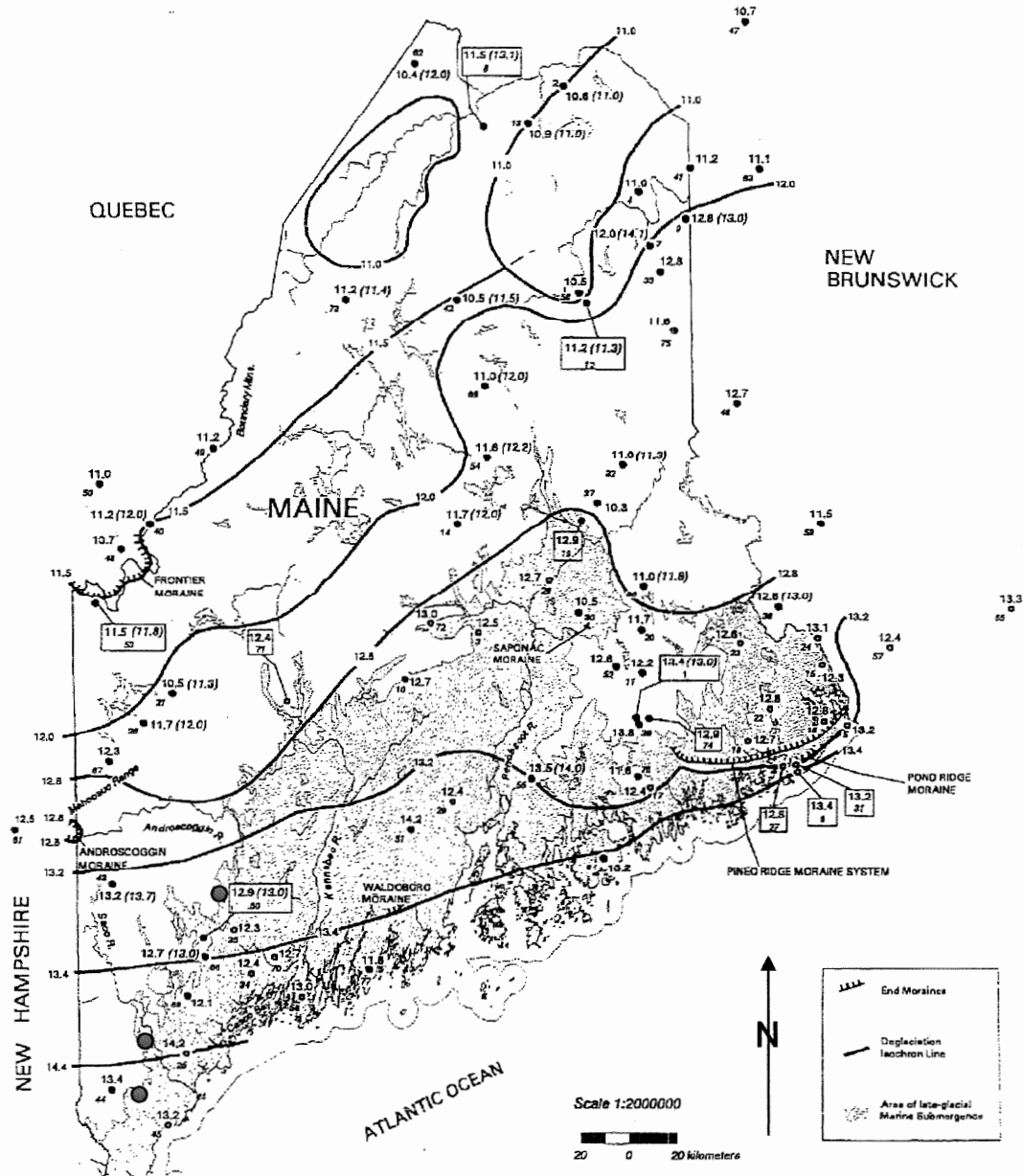


Figure 2.4 Deglacial chronology map of Maine showing deglaciation isochrons estimated from radiocarbon ages taken from marine and terrestrial samples. The isochrons are best fit lines based on the majority of ages and field evidence for the pattern of deglaciation. The major topographic elements such as mountains, basins and end moraines, other ice-contact deposits were all considered in determining the location of the isochrons. Black dots are terrestrial sites that include both the laboratory ages and the estimated time of deglaciation based on pond sediment cores (shown in brackets). Open circles are marine samples that have had a reservoir correction of -600 years applied. All ages are estimated to the nearest 100 years and are in ^{14}C years. Area of late glacial submergence, end moraines and locations of deltas (large orange circles) in the present study are indicated (from Borns et al., 2004).

2.4 Glacial History of southern and coastal Maine

The following is a synthesis of the deglacial history of southern Maine in the region containing the deltas used in the test of TCN dating. The chronology is based on radiocarbon ages provided by Borns et al. (2004), Dorion et al. (2001) and Ridge et al. (2001). During the deglaciation of Maine, from about 17.4 ± 0.5 ka to 11.5 ± 0.3 ka, the Earth's crust experienced residual downwarp (up to 100 m) from the weight of the retreating ice. This and the rising global sea-level due to climate warming led to marine submergence that extended inland from the Maine shelf. Large volumes of sediment were transported to the sea from the melting ice sheet. This sediment was deposited in a variety of glaciomarine features that include the widespread Presumpscot Formation, which formed from the accumulation of silt and clay sized sediment on the ocean floor. Sand and gravel sized sediment built up along the ice margin forming a belt of cross cutting end moraines, ice contact deltas and submarine fans that range from 17.4 ± 0.5 ka to 15.4 ± 0.3 ka (Figure 2.5). Using the deep-sea record, Borns et al. (2004) suggest that much of the coastal moraine belt formed during the Heinrich 1 Event from approximately 18.3 ± 0.3 ka to 16.1 ± 0.5 ka. During this time local glacial advances are believed to have occurred but no evidence for any major regional readvance has been found. The interfingering of glacial and glaciomarine sediments, and the glaciotectonism of glaciomarine sediments indicates that the marine transgression was contemporaneous with the retreat of the ice margin (Thompson et al., 1989). There was variation in the rates of transgression as a consequence of complex competition between glacial-isostatic adjustments and global sea-level rise (Barnhardt et al., 1995).

By 15.2 ± 0.3 ka, the ice sheet had disappeared from central and southern Maine

(Figure 2.6). This revised date is in conflict with earlier dates by Smith (1985) that placed the margin at the coast at this time but is in agreement with varve and other ^{14}C dates in the region (Borns et al., 2004). There was continued transgression up to the marine limit. Isostatic uplift continued after the rate of global sea slowed, which had the effect of raising emerged surfaces from the sea. Deltas and other glaciomarine deposits are now raised and can be used to reconstruct the sequence of deglaciation and marine transgression (Borns et al., 2004).

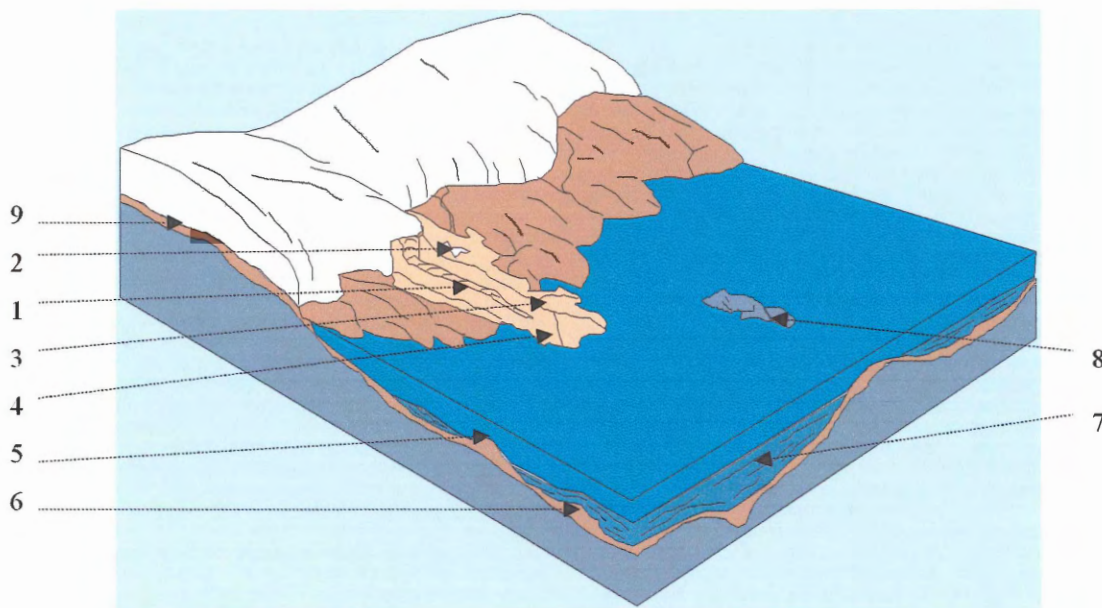


Figure 2.5. The sequence of deglaciation and deposition of surficial materials in southern Maine between ~17.4-15.2 ka. The ice margin fluctuated along the entire coastal zone forming a belt of cross-cutting grounding line end moraines, ice-contact deltas, and submarine fans. The land was still depressed from the weight of the ice, resulting in extensive marine submergence which continued after delta deposition up to marine limit. Marine limits were attained during this period. Much of southern Maine was ice free by ~15.2 ka. The following glacial features are shown: esker (1) and ice block (2) on the outwash plain (3) of the delta (4), end moraines (5), buried end moraines (6), glaciomarine sediments (7), bedrock ridge (8) and till (9) (ages calibrated from Borns and others, 2004; figure modified from Thompson and Borns, 1985b).

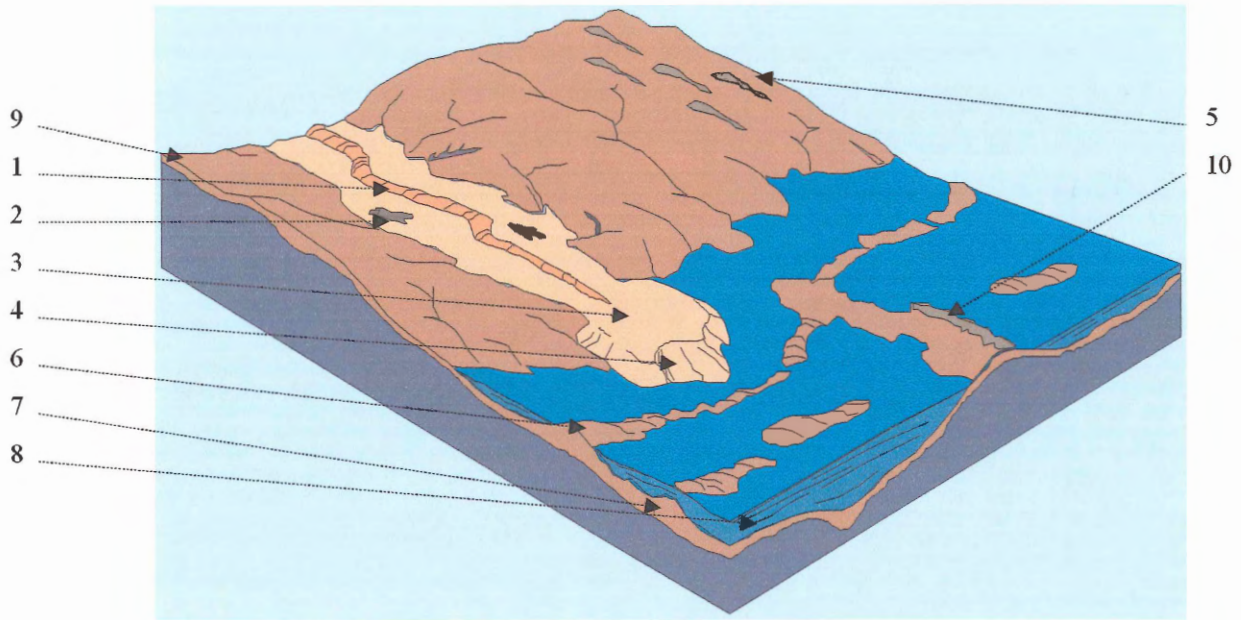


Figure 2.6. The sequence of deglaciation and deposition of surficial materials in southern Maine after 15.2 ka. The ice sheet disappeared from Central Maine. There was continued transgression up to the marine limit. Isostatic adjustment followed, which had the effect of raising the coastal region from the sea so that deltas and other glaciomarine deposits are now raised and can be used to reconstruct the sequence of deglaciation. The following glacial features are shown: esker (1) and kettles (2) on the outwash plain (3) of the delta (4), drumlins (5), end moraines (6), buried end moraines (7), glaciomarine sediments (Presumpscot Formation)(8), till (9) and bedrock ridges (10). (ages calibrated from Borns and others, 2004; figure modified from Thompson and Borns, 1985b).

2.5 TCN Principles

Terrestrial in situ produced cosmogenic nuclides (TCNs) are produced by the interaction between secondary cosmic radiation and exposed target atoms in earth surface materials. It is important to differentiate between those cosmogenic nuclides produced in the atmosphere and subsequently incorporated into earth surface materials from those that are produced in situ in minerals by nuclear reactions arising from radioactive elements. There are six commonly studied in TCNs, the radionuclides ^{10}Be , ^{26}Al , ^{36}Cl , ^{14}C , and the stable noble gases ^3He and ^{21}Ne (Gosse and Phillips, 2001).

The production of cosmogenic nuclides is initiated by primary galactic cosmic radiation (GCR). GCR is composed of highly energetic particles (1-100GeV) that originate mainly from within the Milky Way galaxy (Ligenfelter and Flamm (1964) in Gosse and Phillips, 2001). These particles are composed of 85% protons, 14% α -particles, 3% electrons, and 1% heavier nuclei (Smart and Shea, 1985; Lal, 1988). When GCR reaches the Earth's geomagnetic field, many of the cosmic rays are reflected back into outer-space. The GCR that penetrates the field enters the atmosphere interacts with nuclei of atoms in the atmosphere to produce a cascade of secondary particles that are mostly neutrons and a smaller number of π^\pm and K^\pm mesons (Gosse and Phillips, 2001). Most cosmogenic nuclide production results from neutron spallation reactions where high energy neutrons break up target nuclei. If the mesons do not interact quickly with atmospheric nuclei, they decay to short lived (10^{-6} second lifetime) muons which, like neutrons, also contribute to TCN production. As the secondaries spall with target nuclei, they continue to produce cosmogenic nuclides in the atmosphere, hydrosphere, and lithosphere. Energy is lost due to successive reactions until the neutrons are no longer

capable of causing spallation reactions. Their remaining energy is dissipated through the transfer of momentum to the shattered particles. The cosmogenic nuclide of interest to this study, ^{10}Be , is primarily produced from spallation reactions and muonic interactions with Si and O atoms in quartz.

In situ nuclide production is largely confined to upper 3 m of the Earth's surface (Gosse and Phillips, 2001). Near the surface, close to 98% of the ^{10}Be produced is from spallation reactions involving fast neutrons. Fast neutrons are largely attenuated within depths of 1 to 4 m in bedrock and alluvium. Muons are lighter particles and less reactive and so are able to penetrate to far greater depths (tens of meters) and thus play an important role in producing ^{10}Be below the ground surface.

A TCN production rate is defined as the rate at which a nuclide is produced from a specified element or mineral ($\text{atom g}^{-1} \text{yr}^{-1}$). The production rate for ^{10}Be is the rate at which cosmic radiation produces ^{10}Be in quartz. The average production rate for ^{10}Be is $5.1 \pm 0.3 \text{ atom g}^{-1} \text{yr}^{-1}$ at sea-level (Gosse and Stone, 2001). The concentration of a TCN is affected by the decay of the nuclide. In the case of ^{10}Be , the half life is 1.5 Myr (Yiou and Raisbeck, 1972, Hofmann et al., 1987, Holden, 1990, Middleton et al., 1993 in Gosse and Phillips, 2001). The production of TCN from spallation reactions decreases exponentially with depth below the surface of an exposed landform (Figure 2.7). It can be calculated using the following equation from Gosse and Phillips (2001):

$$P = P_o e^{-d\rho/\Lambda} \quad \text{Equation 2.1}$$

where P is the production rate ($\text{atom g}^{-1} \text{yr}^{-1}$) at a certain depth, P_o is the production rate at the surface ($\text{atom g}^{-1} \text{yr}^{-1}$), d is the depth of the sample (cm), ρ is the bulk density of the rock or sediment (g cm^{-3}), and Λ is the apparent attenuation length (g cm^{-2}).

TCN production rates are dependent on several factors including: geomagnetic latitude, elevation, topography, sample thickness, and depth. Changes in the Earth's geomagnetic field and regional atmospheric pressure anomalies affect long term nuclide production rates creating the largest source of uncertainty in production rates. Due to the primarily dipole geometry of the geomagnetic field, there is an increase in cosmic ray flux towards the poles. This is because the field line orientation relative to the primary radiation varies from transverse at lower latitudes to sub-parallel at the poles (Gosse and Stone, 2001). Thus, production rates are greater at higher latitudes. Production rates also increase with elevation because there is less attenuation by atmospheric gases of the cosmic ray flux at higher altitudes. Cosmic radiation may also be shielded by topography. The presence of mountains would block a portion of the cosmic ray flux, further reducing the production rate at the surface (Gosse and Phillips, 2001).

Within any landform surface, the concentration of TCN is a function of exposure time, erosion rate, burial history, and the initial concentration of nuclides in minerals making up the surface. All of the above factors must be taken into account to determine meaningful exposure ages.

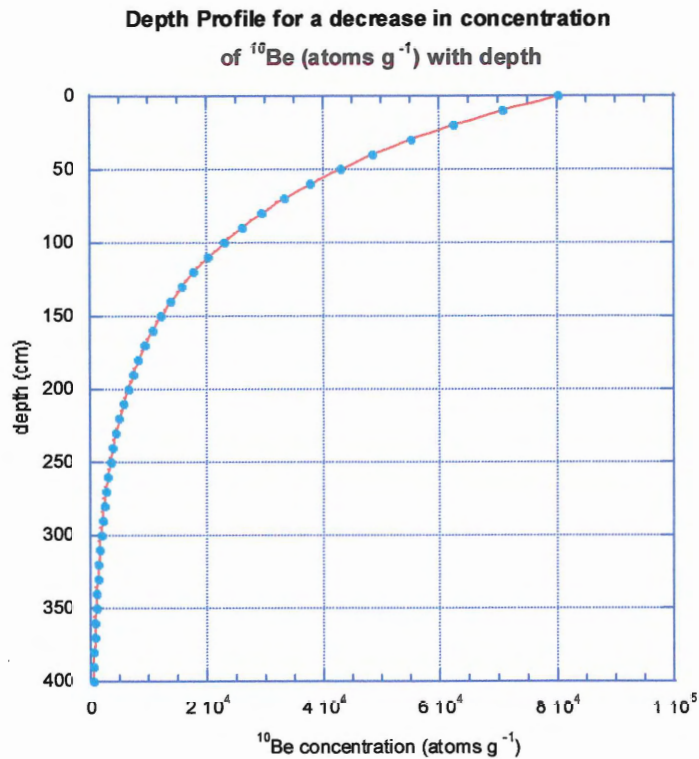


Figure 2.7 Theoretical depth profile for a decrease in concentration of ^{10}Be (atom g^{-1}) with depth (cm) for Auburn Plains Delta, Maine at elevation 113 m. The production rate at this latitude and elevation is $5.35 \text{ atom g}^{-1} \text{ yr}^{-1}$, with a bulk density of 2.0 g/cm^3 and an attenuation length of 150 g cm^{-2} . This curve assumes that there is no inheritance and approaches zero concentration with depth. The production rate has not been adjusted for changes due to sea-level fall or changes in the atmosphere during glacial times.

3. Methodology

3.1 TCN dating of Deltas

TCN dating has been used to solve a broad range of geomorphic and geochronological problems primarily using boulders and bedrock surfaces as media for sampling. Since the early 1990's there have been a growing number of studies that have used TCN dating to date alluvial deposits and other allochthonous landforms. A review of previous applications as well as the principles and methods of TCN dating is provided in Gosse and Phillips (2001). The present investigation is the second known study to date deltaic sediment. The first study by Hilchey (2004) dated deltaic sediment from glaciolacustrine deltas in the Ravn River Valley on Baffin Island (Hilchey, 2004).

The concentration of TCN typically decreases with depth in sedimentary deposits, similar to bedrock. Several specific considerations must be made when sampling sediment. Sediment is subject to vertical mixing near the surface by cryoturbation, bioturbation, and pedoturbation. Samples should be selected below the mixing zone, where sedimentary structures or pedogenic features indicate that there has been no mixing. When sampling Beneath forested surfaces, samples should be taken from below the tree rooting depth, which may be greater than 100 cm depth.

Allochthonous sediments may acquire TCNs that contribute to its inherited concentration at different times throughout their history (Figure 3.1). There may be an inherited concentration from a previous transport-depositional cycle. Inheritance may also be acquired through both exhumation and transport of the sediment to its final site of deposition. Any two clasts (pebble, cobble, sand grain) within a deposit are likely to have different inherited concentrations but a measurement of a large number of clasts

should constrain the mean inheritance (Anderson et al., 1996). Following deposition, accumulation of any TCNs depends on erosion, depth of the sediment and the bulk density of the overlying deposit. The total TCN concentration will include both the inherited component and the TCNs that have accumulated since deposition (Anderson et al., 1996).

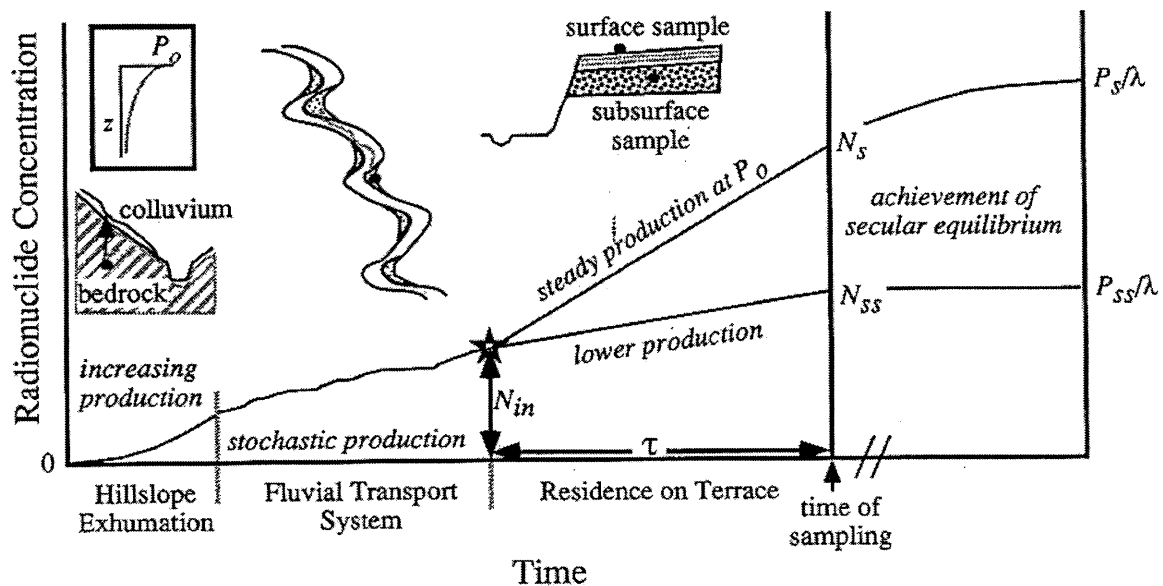


Figure 3.1 TCN concentration history of a clast through its transport history. The inset on the left shows how the production rate changes with depth below the surface. Once the clast is exhumed on the hillslope it starts its transport through the fluvial system. Production during this transport is stochastic as the clast travels between point bars where it is buried to different depths until the clast arrives to the site of final deposition. Evolution of TCN concentration is shown for two different depths, one at the surface and one below. The sample below the surface will have lower production rates. Secular equilibrium is attained for those clasts that are much older than nuclide half lives (from Anderson et al., 1996).

Inheritance can be estimated by collecting surface samples in proximal modern sediments such as modern shorelines, active floodplains or washes that share the same catchment as the sediment being dated. If the sediment has inheritance from previous periods of exposure, then the TCN concentration will exponentially decrease with depth

to its inherited value instead of zero (Gosse and Phillips, 2001).

Another method of measuring inheritance is to collect samples that are well below the penetration depth of fast neutrons, where the sediment has remained shielded. This method assumes that the shielded sediment was deposited at approximately the same time as the overlying sediment during the same depositional event. The amount of inheritance in the deeper sediment may, however, also be greater or less than the inheritance in the shallower sediments (Gosse and Phillips, 2001)

Concentration depth profiles can be constructed by measuring concentrations of multiple samples collected at different depths along a vertical section. Figure 2.7 shows the theoretical depth profile for ^{10}Be in an ideal deposit assuming a single constant exposure and little erosion. The TCN concentrations should decrease exponentially with depth. Samples containing inheritance will have anomalously greater concentrations than the others for a given depth (best fit curve will be displaced to the right) and may not define a simple exponential equation unless the amount of inheritance was uniform with depth (Gosse and Phillips, 2001).

Anderson et al. (1996) constructed depth profiles to constrain inheritance and date sediment in terraces. Each profile included two amalgamated samples, each consisting of 30 clasts, one from the surface and one from a fixed depth in the subsurface. They used the measured inheritance to estimate minimum exhumation rates and maximum transport times (Anderson et al., 1996). That study showed that TCN depth profiles are useful to overcome inheritance problems but they are also powerful tools that can provide information on geomorphic history and processes.

3.2 Site Selection

Three deltas located adjacent to the marine limit in Southern Maine were sampled for TCN dating. The goal was to determine the age of each delta surface. The deltas were selected because they are close to the marine limit, well studied, and formed thick sediment exposures in gravel pits that show little evidence of disturbance evidenced by soil profiles that appear intact below the tree rooting depth and stone fences along the pit boundaries (Thompson, 1982; Thompson and Borns, 1985b; Thompson et al., 1989; Koteff et al., 1993). The stone fences are important because they represent old property boundaries where we can assume there has been little activity (ploughing, excavation) since they were emplaced. The deltas appear flat and well-drained with little evidence of gullying suggesting little surface run-off. The soils seem intact with an observable A and B horizon. The presence of sedimentary structures indicates that the topset-foreset contact is still intact.

Eleven samples were collected following the guidelines set out in Gosse and Phillips (Sections 4.1- 4.4 (2001)). Assuming that inheritance is either negligible or measurable, the exposure ages determined for the delta foresets represent the time that the delta surface was abandoned and hence, the age of the paleo-sea-level. The ages also give an estimate of the timing of deglaciation in the region because all three are ice contact deltas. In order to measure any inheritance, samples were collected over a range of depths, from 1 to 3 m, in a vertical section, below the mixing zone. It was expected that the samples in the vertical sections would have approximately the same age because the deltas were most likely built from eskers over very short periods of time. One kg of sand was used instead of cobbles because the smaller grains present in the sand

considerably reduces variation in the overall mean inheritance of the multiple samples from each delta. Sample information is included in Table 3.1.

3.3 Sample preparation and calculations

3.3.1 Physical pre-treatment

Physical sample preparation, performed in the Crystal Isolation Facility at Dalhousie University, included crushing, milling and sieving following the DAL-CNEF lab procedure. Fractions with a 355-500 grain size were considered the optimal grain size. Fractions with 250-355 grain size were also used when larger amounts of sample were required.

3.3.2 Chemical pre-treatment

Chemical pre-treatment was performed in the Cosmogenic Nuclide Extraction Facility (CNEF) at Dalhousie University. Up to 600 g of sample was mixed with a highly oxidizing aqua regia solution (mixture of 3HCl: 1HNO₃) and heated to 200°C for 2 hours. Aqua regia allowed many of the non-quartz minerals to weaken and dissolve and break up the aggregate grains. From this stage on, only distilled water was used to minimize the introduction of Be and B.

The samples were then etched with a concentrated reagent grade hydrofluoric acid (HF) at 200°C for 30 minutes. HF etching dissolved many of the unwanted mineral grains and stripped off the outer layer from each quartz grain, removing any atmospheric and meteoric cosmogenic ¹⁰Be. Magnetic minerals were removed using a strong bar magnet.

Following HF etching, samples underwent several ultrasonic leaching cycles. The cycles started with higher acid ratios, eg. 240 mL HF: 50 mL HNO₃: 4000 mL H₂O. Less acid was added with additional cycles as the sample was reduced in size and more purified. These cycles were repeated until most of the non-quartz minerals were removed and only a quartz concentrate remained.

To ensure that samples had less than 100ppm of aluminium, Al tests were conducted on 1g samples that was dissolved in HF and then redissolved in 0.5HCL. A Quant-EM stick Al test strip kit was then used to calculate the Al concentration. Those samples with Al concentrations less than 100 ppm were ready for the next phase. Those samples with higher concentrations underwent further chemical pre-treatment that was sample dependent and included some combination of HF etching, ultrasonic leaching or abrasion before being Al-tested again.

3.3.3 Quartz dissolution

0.3 ml of 1000 ppm Be carrier was added to each quartz concentrate sample (up to 120 g). The carrier is mostly ⁹Be with a known amount of ¹⁰Be that is used to give the AMS a larger target for analysis. The ⁹Be mass must be measured to 4 decimal places. This can only be accomplished by adding a large amount of carrier gravimetrically. A geochemical blank was also prepared to which only carrier was added without quartz. Samples and blanks were dissolved in 120ml HF, 12ml HClO₄, and 25 ml aqua regia. The samples went through a series of dissolutions and evaporations until only Be₂O₃ remained. Appendix 1 provides an outline of all chemistry steps taken.

3.3.4 Ion chromatography

Samples were then redissolved and placed in an anion exchange column that contains microscopic spheres of styrene resin with high exchange capacities allowing unwanted elements to be removed. Anions in the sample solutions were either adsorbed onto or substituted into the resin spheres. By controlling the pH of the columns, it was possible to control which anions were collected by the resin. BeCl_2 and AlCl_3 passed through the columns at 9N HCl and were collected as eluant for the following steps.

A controlled precipitation was conducted to separate unwanted elements that precipitate as hydroxides from other elements. NH_4OH was added to the sample solutions. At pHs of 6.5 –9.5, hydroxides were precipitated. $\text{Be}(\text{OH})_2$ is insoluble at these pHs.

Samples were then placed in pH-controlled cation columns to separate Be from all remaining elements by ion chromatography. Unwanted cations were collected and discarded and Be and Al eluants were concentrated and collected separately. The Be eluant underwent more dissolution and evaporations and precipitation using ultra pure ammonia gas. These processes converted the BeCl to BeOH that was then baked in quartz vials at 850°C leaving an oxide powder (approximately 1 mg) that was packed into special target holders with a niobium powder and then sent to Lawrence Livermore Laboratory for AMS.

3.3.5 AMS and data reduction

AMS measures the isotopic ratio of stable and cosmogenic Be isotopes. The $^{10}\text{Be}/^9\text{Be}$ ratios of the samples and blanks were measured with acceptable precisions. The

amount of ^{10}Be was calculated using the following equation from Gosse and Phillips (2001):

$$^{10}\text{Be} = R_{[10/9]} m^c \left[N_A / A_{\text{Be}} \right] / m_{\text{qtz}} \quad \text{Equation 3.1}$$

Where:

$^{10}\text{Be} = \text{atom g}^{-1}$

$R_{[10/9]} = ^{10}\text{Be}/^9\text{Be}$ ratio

$N_A = \text{Avogadro's number}$

$A_{\text{Be}} = \text{Atomic weight of Be}$

$m_{\text{qtz}} = \text{mass of quartz (g)}$

$m^c = \text{mass of carrier (g)}$

Before calculating the exposure ages, the production rates were calculated taking into account latitude, elevation, depth, sample thickness, and bulk density. Inheritance adjustments were determined and applied to the ages. Inheritance was estimated by using a least-squares regression method to minimize the standard deviation among the sample concentrations. The effects of snow and tree cover were estimated. Effects on production rates of the isostatic uplift (>110m) since deglaciation were also determined. A sensitivity analysis examined the effects of density and erosion on exposure ages.

Two samples (one from Dayton delta and one from Jailhouse delta) were reanalyzed separately to determine if there was an AMS or chemical error. Those samples affected by the suspected error were excluded from age determinations and adjustments.

3.4 Age comparisons

The calculated TCN ages were then compared to radiocarbon ages taken from the radiocarbon ages compiled by Borns and others (2004). Factors effecting both TCN and ^{14}C ages were investigated to try understand the obtained ages.

Sample ID	CNEF ID	Material sampled	Depth (cm)	Sample Thickness (cm)
Auburn Plains Delta				
ME-02-APD-101	1229	topsets	94	4.0
ME-02-APD-102	1230	foresets	135	5.1
ME-02-APD-103	1231	foresets	174	7.6
ME-02-APD-104	1232	foresets	215	12.7
ME-02-APD-105	1233	foresets	265	7.6
Jailhouse Delta				
ME-02-JHD-109	1236	foresets	82	3.8
ME-02-JHD-110	1237	foresets	115	3.8
Dayton Delta				
ME-02-DAY-112	1238	foresets	117	5.1
ME-02-DAY-113	1239	foresets	193	5.1
ME-02-DAY-114	1240	foresets	251	2.5
ME-02-DAY-115	1241	foresets	307	2.5

Table 3.1. Sample Information for samples from Auburn Plains Delta, Jailhouse Delta, and Dayton Delta. Auburn Plains delta is 44.17°N, 70.24°W at 113m elevation. Jailhouse delta is 43.46°N, 70.72°W at 84m elevation. Dayton delta is 43.54°N, 70.6°W at 91m elevation. All three deltas are less than 2 km below the marine limit. Elevations measured using GPS are not exactly at topset-foreset contact.

4. Results

4.1 ^{10}Be concentrations

Eleven samples from three delta profiles were analyzed. All samples were analyzed with a chemical blank (seven samples per blank) in order to indicate the AMS and geochemical background. The blank analyzed with the samples from Auburn Plains Delta was 11.9×10^4 ^{10}Be atoms. The chemical blank analyzed with the samples from Dayton and Jailhouse Delta was 43.5×10^4 ^{10}Be atoms. This blank is anomalously high (by an order of magnitude) and suggests an AMS or geochemical error. A typical blank is approximately 9.50×10^4 ^{10}Be atoms. AMS worksheets are provided in Appendix 2.

The concentrations of the samples from the Auburn Plains delta profile range from 34.6×10^3 ^{10}Be atom g^{-1} quartz (shallowest) to 17.2×10^3 ^{10}Be atom g^{-1} quartz (deepest). The concentrations of the samples from the Dayton delta profile range from 7.5×10^3 ^{10}Be atom g^{-1} quartz to 12.8×10^3 ^{10}Be atom g^{-1} quartz. The concentrations of the two samples from the Jailhouse Delta profile (starting with the shallowest sample) are 24.8×10^3 ^{10}Be atom g^{-1} quartz and 30.0×10^3 ^{10}Be atom g^{-1} quartz. Table 4.1 shows the ^{10}Be concentrations for the three delta depth profiles.

Figure 4.1 shows the change in ^{10}Be concentrations with depth for the five samples from Auburn Plains delta. From this figure, one outlier is apparent. Figure 4.2 more clearly shows the relationship between the remaining four samples once this outlier is removed. This curve shows a near exponential decrease in concentration with depth. The four samples in the Dayton Delta profile (Figure 4.3) show no observed trend of exponential decrease in concentration with depth. The ^{10}Be concentrations increase with depth, contrary to what was expected. The two samples from Jailhouse delta profile

(Figure 4.3) also show increased ^{10}Be concentration with depth. However, with only two data points, we cannot discern whether this delta profile is showing any trend of increase or decrease with depth.

Because of a suspected AMS or chemical error, ages were not determined for these samples and two of these samples (one from each delta) were reanalyzed. Careful examination of the AMS analysis showed that other samples that were concurrently run with those from Jailhouse delta and Dayton delta had reasonably low blanks and low AMS uncertainty. There does not appear to have been any AMS error in the batch of samples, suggesting that there was a geochemical error in processing the Jailhouse and Dayton delta samples.

The concentrations of the two samples that were reanalyzed, sample 1237 from Jailhouse delta and sample 1241 from Dayton delta are shown in Table 4.1. The ^{10}Be concentration of sample 1237 is similar to the first analysis, 30.0×10^3 versus 31.8×10^3 ^{10}Be atom g^{-1} of quartz. However, sample 1241 from Dayton delta gave a much higher concentration than the first analysis. Based on these differences in concentrations, we are fairly confident that there has been a geochemical error in the first analysis. Not enough data is available to make any interpretation on the reanalyzed samples. Ages and adjustments were not determined for Dayton and Jailhouse deltas.

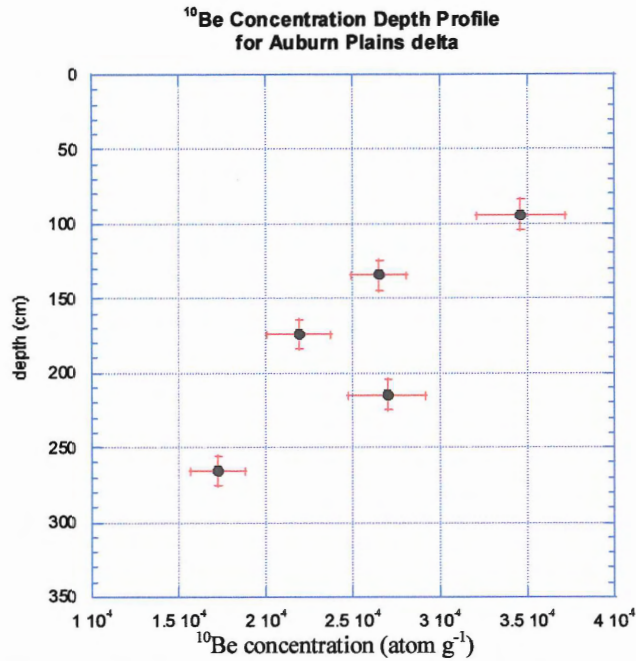


Figure 4.1. ^{10}Be concentrations for all samples from Auburn Plains Delta. No adjustments for inheritance were applied to these concentrations. Errors from depth measurements are shown in the vertical error bars. The AMS uncertainty is shown in the horizontal error bars.

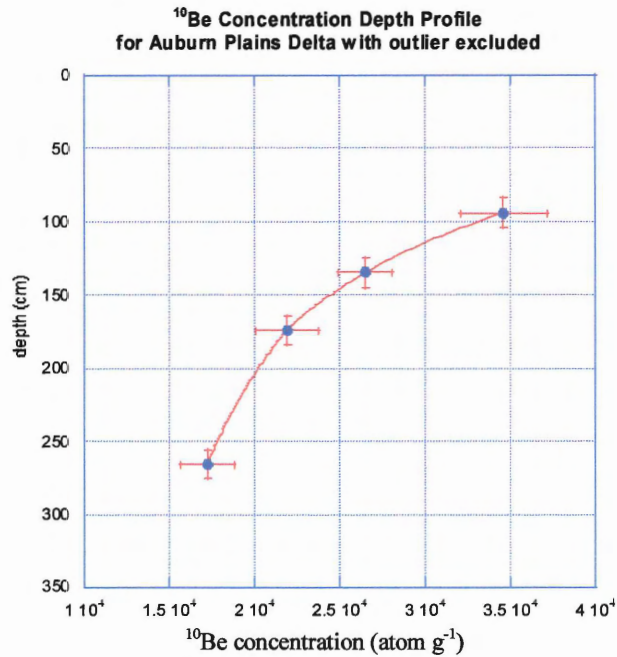


Figure 4.2 ^{10}Be concentrations for four samples from Auburn Plains Delta, excluding the outlier. No adjustments for inheritance were applied to these concentrations. The ^{10}Be concentrations show an exponential decrease with depth ($r^2 = 0.96$).

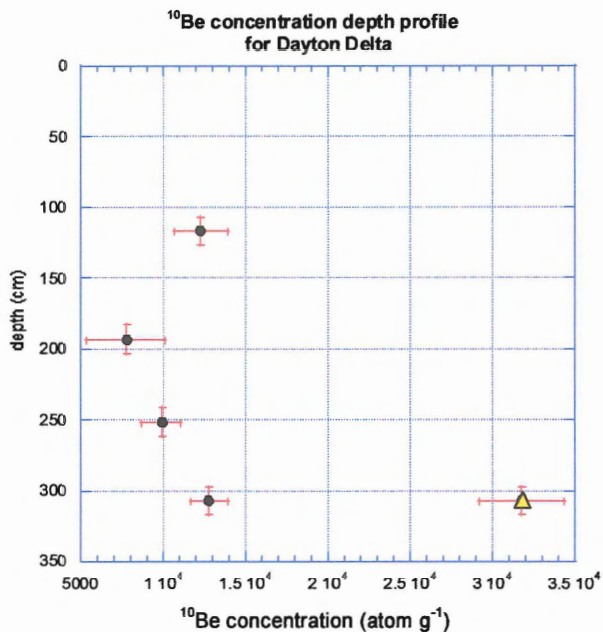


Figure 4.3. ¹⁰Be concentrations for four samples from Dayton delta. No adjustments for inheritance were applied to these concentrations. The ¹⁰Be concentrations do not show an exponential pattern of decrease in concentration with depth. The reanalyzed sample is also shown (Δ).

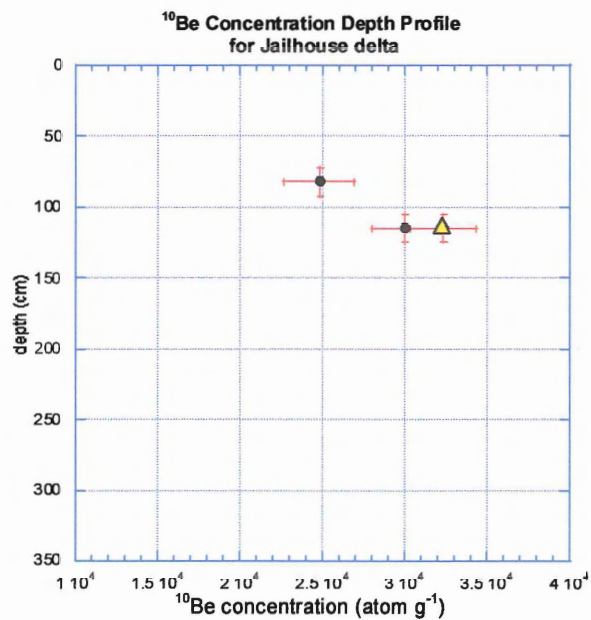


Figure 4.4. ¹⁰Be concentrations for samples from Jailhouse Delta. No adjustments for inheritance were applied to these concentrations. The ¹⁰Be concentrations do not show an exponential pattern of decrease in concentration with depth. The reanalyzed sample is also shown (Δ).

12/10/11

Sample ID	CNEF ID	Depth (cm)	¹⁰ Be concentration		Production rate atom g ⁻¹ yr ⁻¹	Age		Inheritance atom g ⁻¹	Inheritance-adjusted Age	
			10 ⁴ atom g ⁻¹	uncertainty (%)		ka	uncertainty (ka)		ka	uncertainty(ka)
Auburn Plains Delta										
ME-02-APD-101	1229	94	3.46	3.8	1.81	19.2	1.4	14594	11.0	0.8
ME-02-APD-102	1230	135	2.65	3.0	1.14	23.3	1.4	14594	10.5	0.6
ME-02-APD-103	1231	174	2.19	4.3	0.72	30.6	2.6	14594	10.2	0.8
ME-02-APD-104	1232	215	2.69	4.2	0.44	61.8	5.0	14594	28.2	2.3
ME-02-APD-105	1233	265	1.72	4.7	0.26	67.9	6.2	14594	10.3	0.9
mean						40.6	22.6		14.0	7.9
Jailhouse Delta										
ME-02-JHD-109	1236	82	2.48	4.3	2.02	12.3	1.0			
ME-02-JHD-110	1237	115	3.00	3.4	1.39	21.7	1.4			
ME-02-JHD-110 (2 nd)	1237	115	3.23	3.1	1.39	23.3	1.4			
Dayton Delta										
ME-02-DAY-112	1238	117	1.23	6.9	1.40	8.8	1.2			
ME-02-DAY-113	1239	193	7.75	15.6	0.61	12.8	3.9			
ME-02-DAY-114	1240	251	9.88	6.3	0.32	30.7	3.8			
ME-02-DAY-115	1241	307	1.28	4.5	0.18	74.1	6.5			
ME-02-DAY-115 (2 nd)	1241	307	3.18	4.1	0.18	189.2	15.4			

Table 4.1. TCN concentrations, exposure ages, and inheritance calculated for samples from 3 deltas. ¹⁰Be concentrations measured by AMS and the AMS uncertainties (2σ) are shown. The site production rates were calculated using the production rate at sea level (5.1 ¹⁰Be atom g⁻¹ yr⁻¹), the elevation of the delta, the latitude (included in Table 3.1), the attenuation length (Λ) of 160 g cm⁻², density of 2.0 g cm⁻³, and depth below the surface (cm). Ages and inheritance-adjusted ages are reported at 2σ. Sample 1232 (outlier) was excluded from inheritance-adjustments and was not included in the mean age. Ages and inheritance adjustments were not determined for Dayton delta and Jailhouse delta due to suspect geochemical error. The reanalyzed samples are indicated with a (2nd).

4.2 Interpretation of concentrations as ages

The ages of the five samples from Auburn Plains Delta (Table 4.1) range from: 19.2 ± 1.4 ka to 67.9 ± 6.2 ka. In all instances here and below, a 2σ AMS precision is shown for an individual age, but for mean ages two standard deviations about the mean age are shown, with a coefficient of variation at 2σ expressed in percentage. A thorough discussion of sources of error will be provided below. The delta age is assigned by averaging the ages for all the samples within the profile. The mean age for the Auburn Plains delta is 40.6 ka \pm 45.2 ka (2 standard deviations about the mean), with a coefficient of variation of 112%. This age is older and more scattered than that expected based on the radiocarbon chronology, suggesting that inheritance has been a significant contributor.

4.3 Inheritance Adjustments

The ages reported above were determined assuming that there is no inheritance. The total concentration of any sample includes both the TCNs accumulated prior to deposition (inheritance) and the TCNs accumulated following deposition. In determining inheritance, several assumptions were made: the inherited concentration should be equal throughout the deposit and is not a function of depth within the deposit, deposition was rapid relative to the age of the deposit, and the TCN concentrations should follow an exponential profile (as shown in Figure 2.7) (Anderson et al., 1996; Hancock et al., 1999). Inheritance was estimated for Auburn Plains delta using a least-squares regression method to minimize the standard deviation among the samples. Only four of the five samples were used because sample 1232 is considered a statistical outlier as its concentration falls outside the 2σ uncertainty range of all other concentrations in the

depth profile. The inheritance-corrected concentrations are shown with the uncorrected concentrations in Figure 4.5. The calculated inheritance correction for the samples from Auburn Plains Delta is 1.46×10^4 atom g^{-1} (Table 4.1).

It is difficult to assign an uncertainty to the inheritance adjustment. Therefore a range of inheritances can be used to establish the plausibility of other inheritance values. Figure 4.7 shows how the exposure ages would vary over a range of inheritance values. The ages at different depths in the profile should be approximately equal to each other because of rapid deposition of the delta. Inheritance values of 1.4×10^4 to 1.5×10^4 atom g^{-1} provide reasonable constraints on the age of the delta. Outside of this range there is more scatter in the ages that results in anomalous age profiles.

The inheritance-adjusted exposure ages range from 10.1 ± 0.8 ka to 11.1 ± 0.8 ka (excluding the outlier) (Figure 4.6). The mean inheritance-adjusted exposure age of Auburn Plains Delta, taken from the average of four of the five samples (outlier excluded), for a constant inheritance, is 10.5 ± 0.4 ka. The variance among these samples, which is controlled by all sources of random error, is $\sigma^2 = 0.9$ ka, or a coefficient of variation of 7.6% at 2σ . The variance can be completely explained by the AMS uncertainty, which may imply that the other sources of random error are small. The unadjusted ages do not have a simple exponential concentration profile with an attenuation length (Λ) of 160 g cm^{-2} (Figure 4.5). With the application of inheritance adjustments, there is excellent agreement among four of the five samples, decreasing the coefficient of variation from 112% (unadjusted ages) to 7.6% (adjusted ages). The adjusted mean age must be interpreted as a minimum age of delta deposition as there have been no corrections made for snow, water, erosion, soil mixing, burial, and

vegetation.

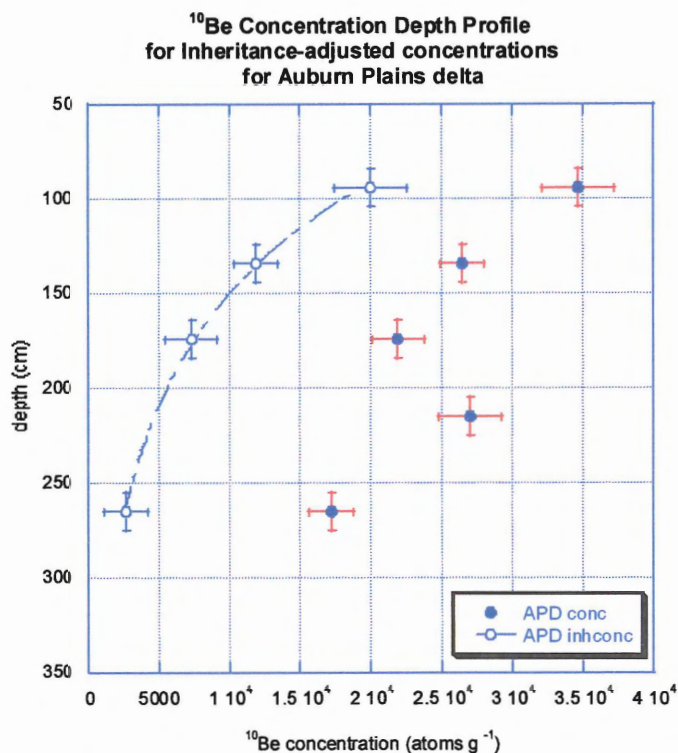


Figure 4.5. Inheritance-adjusted concentrations for Auburn Plains Delta, excluding the outlier. The curve for the adjusted ^{10}Be concentrations shows an exponential decrease with depth ($r^2 = 0.96$). The unadjusted concentrations are shown on the right for comparison. An inheritance value of 1.46×10^4 atom g^{-1} was estimated using a least-squares regression method to minimize the standard deviation among the samples.

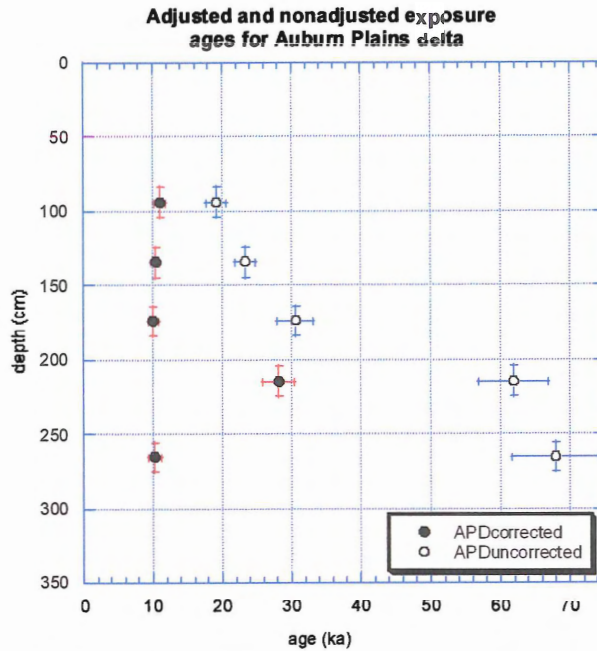


Figure 4.6. Exposure ages for Auburn Plains Delta. The inheritance adjusted ages, excluding the outlier, have a mean age of 11.0 ± 0.9 ka. The unadjusted ages are shown on the right for comparison.

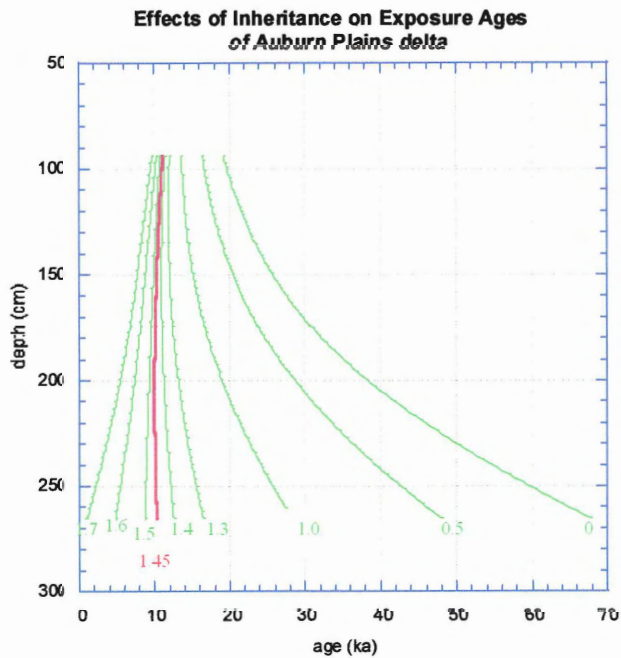


Figure 4.7 Effects of Inheritance on exposure ages of Auburn Plains delta. The green curves show the effect of different inheritance values on exposure ages. Inheritance values are shown as 10^4 atom g^{-1} . The red curve shows the inheritance value of $14594 \text{ atom g}^{-1}$ used in all calculations.

4.4 Uncertainties

The total uncertainty in any calculated age can be reported as:

$$(\Sigma(\text{random errors}^2 + \text{systematic errors}^2))^{1/2} \quad \text{Equation 4.1}$$

Systematic uncertainties influence the accuracy of calculations. The greatest source of error is from estimates of production rates. Other sources of error include: temporal variations in production rates, carrier and standards, and other calculation errors. The average Poisson precision in the $^{10}\text{Be}/^9\text{Be}$ by AMS is <5% at 2σ , a range appropriate for this test (Gosse and Phillips, 2001). Random errors influence the precision of the ages. Potential sources of random error in dating deltas may arise from inheritance adjustments, erosion of the delta topsets, wave reworking of sediment, soil mixing, soil density estimates, sample thickness measurements, water and snow cover as well as burial. Overall, the average random uncertainty for ages in the deltas is within 8 % (2σ). The coefficient of error about the mean includes both systematic and random sources of error giving a total uncertainty for the exposure age in Auburn Plains delta of 16% (2σ).

4.5 Adjustments for other factors

4.5.1 Tree Cover

The effect of tree cover on the cosmic ray flux is presently being studied for old growth forests in Nova Scotia. The forest types in Nova Scotia are similar to those in Maine and include mixed deciduous, coniferous, boreal forests. The mean flux was calculated over 221 old growth plots (10 sample locations per plot) in Nova Scotia. These results show that there is a tree cover effect of $3.0 \pm 0.2\%$ (Gosse and Plug, in

prep.) which means the production rate assumed is overestimated by 3%. The mean age should therefore be increased by 0.3 ka to 10.8 ± 0.8 ka (2σ).

4.5.2 Production Rates

Age calculations were made using production rates that assume the surface of Auburn Plains delta was at its present elevation of 113 m above sea-level. Auburn Plains delta was deposited at sea-level as the ice sheet retreated. There has been at least 113 m of relative sea-level fall since deglaciation. All of this sea-level fall can be attributed to isostasy. Following deglaciation, isostatic uplift of the land was fastest during the first few thousand years (Peltier, 1998). Sea-level was also rising during the first few thousand years of exposure from melting of the ice sheet. This increased rate of sea-level rise is shown in the Barbados sea-level curve (Figure 4.8). Isostatic uplift eventually outpaced sea-level rise. The present elevation of Auburn Plains delta is a function of a combination of isostatic uplift and sea-level change. The production rates used in the age calculations did not take this relative sea-level change into account. I calculated a half response time of 1550 years to simulate the relative sea-level fall. The 1550 year half response time was estimated by using the exponential nature of postglacial rebound and the present elevation as the final elevation over a 14000 yr period. Using this half response time, the time integrated (apparent) production rate on a rising surface was calculated over 14 ka (Figure 4.9, Table 4.2). The result shows that the production rates should be reduced by 1.6%. The adjusted age is 11.0 ± 0.9 ka (2σ).

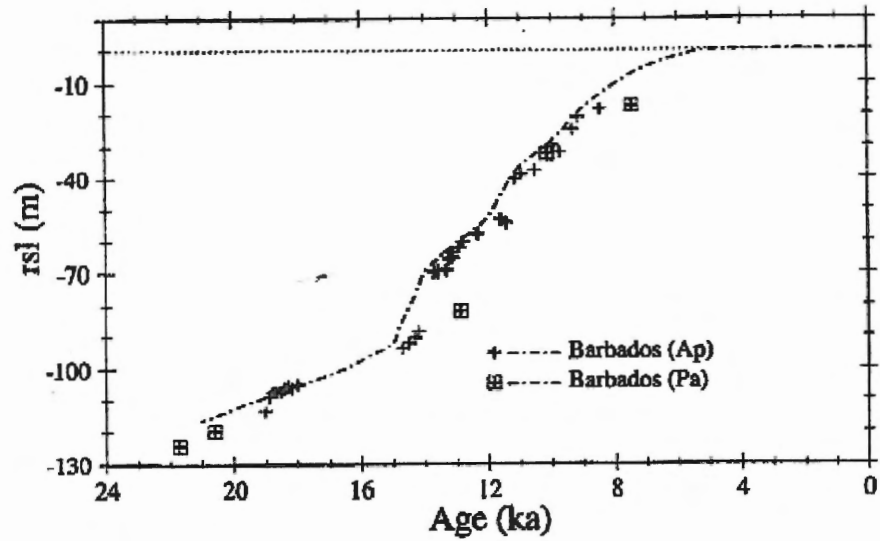


Figure 4.8 Postglacial relative sea-level change curve at Barbados, which extends from the Last Glacial Maximum (LGM). This curve is based on the U/Th dated coral-based record. The curve shows that sea-level was depressed by ~120 m at LGM (Fairbanks (1989) in Peltier, 1998).

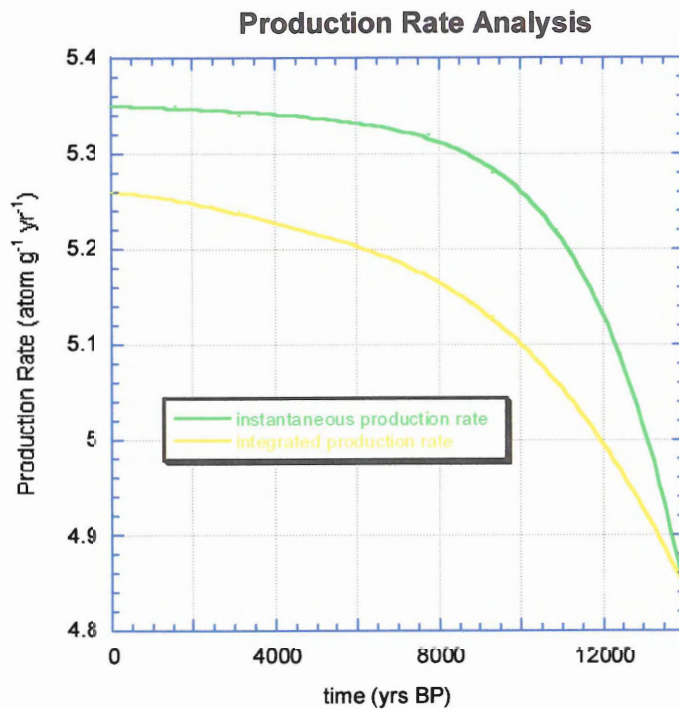


Figure 4.9 The time integrated production rate for Auburn Plains delta over 15 ka where 0 yr is the present. This production rate was calculated using a half response time of 1550 yrs and the present elevation of 113 m at latitude 44.17°. The half response time was calculated using the exponential nature of postglacial rebound and the present elevation as the final elevation over a 14000 yr period. The instantaneous production rate used in the age calculations is also shown.

RUN	model time	Time BP (yr)	Elevation (m)	Instantaneous production rate atom/g/yr	Time integrated production rate atom/g/yr
0	0	13950	0	4.85	4.85
1	1550	12400	57	5.09	4.97
2	3100	10850	85	5.22	5.06
3	4650	9300	99	5.28	5.13
4	6200	7750	106	5.32	5.17
5	7750	6200	109	5.33	5.20
6	9300	4650	111	5.34	5.22
7	10850	3100	112	5.34	5.24
8	12400	1550	112	5.35	5.25
9	13950	0	113	5.35	5.26

Table 4.2 Time integrated production rate ($\text{atom g}^{-1} \text{yr}^{-1}$) for a rising surface that starts at sea-level. The present (final) elevation is 113 m. This production rate was calculated using a half response time of 1550 yrs. The half response time was calculated using the present elevation as the final elevation over a 14000 yr period. The instantaneous production rate does not take the change in elevation into account.

4.5.3 Snow Cover

No direct snow data was available from Auburn, Maine. Snow data covering 1971-2000 from surrounding weather stations in Bangor, Maine (snow fallen) and Vermont (snow fallen and snow depths), provided by the National Oceanographic Atmospheric Administration (NOAA) and the Maine Cooperative Snow Survey, was used to estimate snow depth and the affect of snow cover on the Auburn Plains Delta. All snow data including snow depths and the relationship between snow depth and snow fallen is shown in Appendix 3. Using this relationship the average snow depth was calculated for three months of winter (90 days), averaged over the past 30 years. The median snow depth for Auburn Plains delta is estimated to be 13 cm. The mean snow density is 0.25 g cm^{-3} (Maine Cooperative Snow Survey). Figure 4.9 calculates the effects of shielding by snow of common densities and thickness and assumes a snow cover period of 3 months/year. According to this figure, for a snow depth of 13 cm there is a 0.4% difference from the actual age due to snow shielding. When adjusted for the

effect of snow cover, the mean age is 11.0 ± 0.9 ka (2σ).

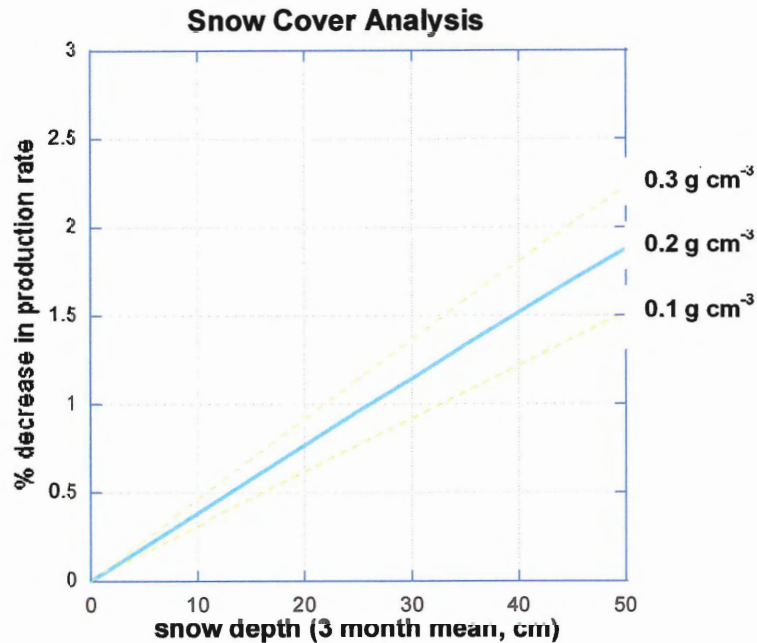


Figure 4.10 Effects on TCN ages by snow cover of common densities and thicknesses. Calculations were made assuming a simple exposure time with snow shielding applied for 4 months each year (modified from Gosse and Phillips, 2001).

4.6 Sensitivity Analysis

4.6.1 Introduction

A sensitivity analysis was performed to determine how the effects of density and erosion would affect the exposure age of Auburn Plains delta. A range of reasonable values for each of these factors was used to determine the effect on the exposure ages. This analysis also provides insight for sampling strategies on other raised deltas and interpretations of exposure ages of deltas. All calculations were made using four of the five Auburn Plains delta samples, excluding the outlier.

4.6.2 Bulk density of the sediments

All samples consisted of fine to medium grained sand. An average bulk density of 2.00g/cm^3 was used in all calculations. Figure 4.10 shows how the ages would change over a range of reasonable densities from 1.7 g/cm^3 to 2.3 g/cm^3 . There is a 1.1 % decrease in age with a density as low as 1.75 g/cm^3 . There is a 1.1 % increase in age with a density as high as 2.25 g/cm^3 . The effect on exposure ages over a range of reasonable densities is small. A density of 2.0g cm^{-3} in the middle of this range is considered to be representative.

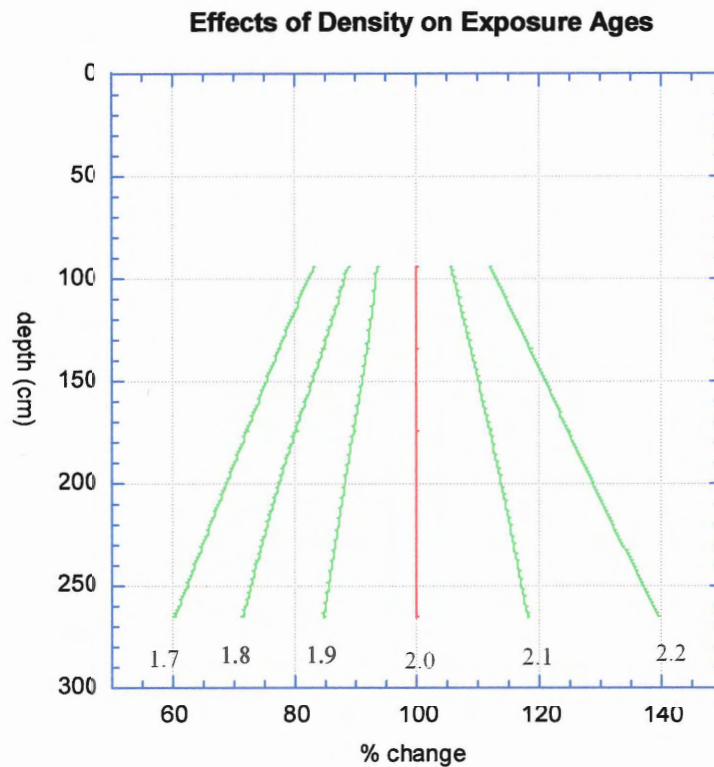


Figure 4.11. Effects on TCN ages by varying the soil density over a range of common densities. Ages have been adjusted for inheritance ($1.46 \times 10^4\text{ atom g}^{-1}$). The outlier has been excluded from this analysis. The red curve shows the density (2.0 g cm^{-3}) used in all calculations. The green curves show the percent change in age for a range of density values, from 1.7 to 2.2 g cm^{-3} .

4.6.3 Erosion

It was expected that erosion since the Holocene should be minimal based on field observations. Sedimentary structures appeared intact and the topset-foreset contact was generally 1 to 2 m below the surface. However, if there was erosion it would result in younger TCN ages. For example, for a 15 ka surface, an erosion rate of 0.035 mm yr^{-1} (removal of 52 cm of sediment in 15 ka) results in a TCN date on Auburn Plains delta of 11 ka (Figure 4.11).

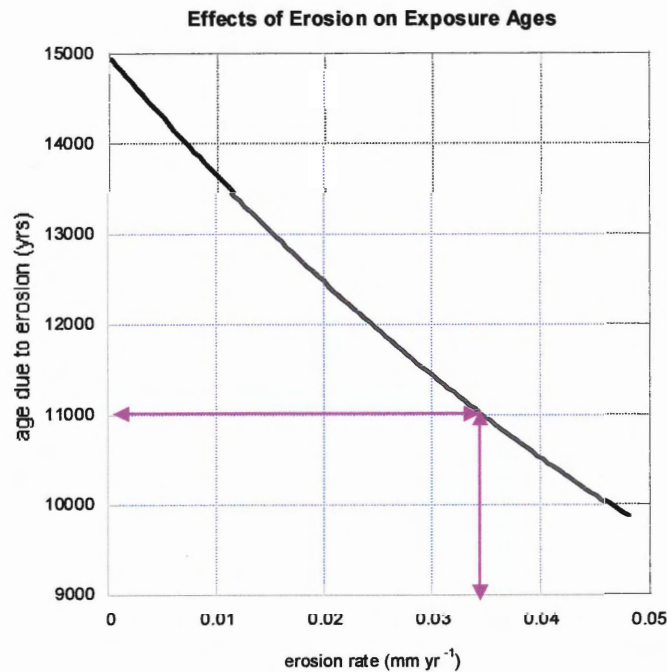


Figure 4.12 Effects of erosion on the exposure age of Auburn Plains delta. For an erosion rate of 0 mm yr^{-1} , the age of the delta is 15 ka. For higher erosion rates, the apparent exposure age of the surface gets younger. The TCN age of Auburn Plains delta is 11.0 ka. An erosion rate of 0.04 mm yr^{-1} or 60 cm in the past 15 ka would be necessary for the exposure age to become 11.0 ka.

5 Interpretations

5.1 Interpretation of the exposure age of Auburn Plains Delta

After all adjustments, the best TCN age for Auburn Plains delta is 11.0 ± 0.9 ka (2σ). This result shows that TCN dating can be used to precisely date deltaic sediment. This age provides a minimum age for the deposition of the delta (at sea-level) at the retreating ice margin. The sensitivity analysis showed that a density of 2.0 g cm^{-3} is reasonable. However, an erosion rate of 0.035 mm yr^{-1} can contribute to explaining the disparity between the TCN ages and the ^{14}C ages. Erosion results in younger TCN ages that provide minimum ages for delta deposition. Over adjustments for inheritance also result in younger TCN ages. In the following sections the implications of the TCN age of Auburn Plains delta will be placed into the regional geological context.

5.2 Accuracy and comparison with pre-existing chronology

The existing radiocarbon dates closest (within 30 km and below the marine limit) to Auburn Plains delta (Figure 2.4) come from six dates obtained from marine shells and terrestrial plant macrofossils that range in age from 14.0 ± 0.2 ka to 15.4 ± 0.4 ka. All radiocarbon dates from Maine are reported in Borns et al. (2004) and those in the Auburn Plains delta vicinity are summarized in Table 5.1. Reservoir corrections of -600 years were applied to the marine ^{14}C ages. The marine ages from *Portlandia arctica* found in the Presumpscot Formation provide close minimum ages of deglaciation because the ice had to be gone in order for the muds and clay to be deposited. The terrestrial ^{14}C ages, inferred from plant macrofossil dates from sediment near the bottom of glacial lakes, also provide a minimum age for the ice margin position at each lake. Because the marine

and terrestrial dates are in reasonable agreement, their average was taken. Auburn Plains delta is up to 30 km northwest of these ^{14}C sample sites. While these ^{14}C ages provide minimum ages for deglaciation they are maximum ages for the age of Auburn Plains delta which was deglaciated later. The mean age of all six radiocarbon dates, 14.7 ± 0.45 ka, represents a maximum age for Auburn Plains Delta. Based on this age, the TCN age of Auburn Plains Delta is approximately 3.7 ka younger than that predicted from the radiocarbon-based chronology.

Site	Lat. (°N)	Long (°W)	Distance (km)	Setting	Material	^{14}C age (ka BP)	Calibrated Age (ka)
34	43.90	70.10	30	Marine	<i>Portlandia arctica</i>	12.4±0.05	14.5±0.3
35	44.06	70.19	12	Marine	<i>Portlandia arctica</i>	12.3±0.08	14.3±0.4
60	44.03	70.35	16	Terrestrial	Plant macrofossils	13.0±0.32	15.2±1.0
66	43.96	70.34	24	Terrestrial	Plant macrofossils	13.0±0.12	15.4±0.4
68	43.82	70.43	40	Terrestrial	<i>Populus balsamifera</i>	12.1±0.11	14.0±0.2
70	43.96	69.98	35	Marine	<i>Portlandia arctica</i>	12.7±0.09	15.0±0.4
							mean: 14.7±0.4

Table 5.1 Radiocarbon ages from Auburn Plains delta vicinity used to establish the deglaciation chronology of Maine (from Borns et al., 2004). These ages are minimum ages for deglaciation but maximum ages for Auburn plains delta. All sites are located south of Auburn Plains delta and were deglaciated earlier.

There are several factors that may explain the difference between the exposure date of Auburn Plains Delta and the expected date of 14.7 ± 0.4 ka from the ^{14}C chronology. Table 5.2 summarizes the most important factors that may explain the difference between the ^{14}C and TCN ages. First, there are important differences between the two dating techniques that have to be taken into consideration. In addition to the discrepancy that still exists between the marine ^{14}C chronology and the terrestrial ^{14}C chronology from varve sequence correlations, ^{14}C dating provides ages from material deposited some time during or after delta deposition making it difficult to uniquely date

an event such as delta deposition. In contrast, TCN dating provides the date since the deltas have been exposed. At the marine limit, where marine submergence reached its greatest extent, exposure ages provide ages that mark the transition from transgression to regression. Therefore, the difference between the ^{14}C and TCN ages may provide an indication of how long it took for the delta to be deposited.

There may have been delayed emergence as a result of isostatic rebound. This effect would be very small for ages at or near the marine limit but would be greater for deltas further below the marine limit. In regions that were occupied by the LIS, the load placed by the ice on the Earth's crust caused the crust to sink down into the underlying mantle, depressing the land surface relative to sea-level. The amount of depression decreases from the centre of the ice sheet towards the ice sheet margin, where the ice is thinner. Because of lithospheric rigidity, a peripheral depression continues beyond the ice sheet margin. During deglaciation and unloading, the lithosphere rebounded beneath the ice sheet (Benn and Evans, 1998).

The research of Koteff and Larsen (1989) suggests that there has been approximately 5 ka delay in isostatic uplift following deglaciation in western New England. These results are supported by studies of glaciomarine delta elevations by Thompson et al. (1989) and Koteff et al. (1993). Thompson et al. (1989) surveyed over 100 glaciomarine deltas in Maine and used the topset-foreset contact elevations and dip directions to measure the pattern of post-glacial crustal uplift and tilt. The isostatic uplift pattern suggests that the LIS radiated across Maine from a spreading center in the direction of southern Quebec. Koteff et al. (1993) also used delta elevations and dip directions to add to this work, confirming this delayed postglacial uplift model of ~ 5 ka

after the onset of deglaciation. This theory of delayed uplift would result in delayed emergence of the deltas that would provide younger TCN ages but have no effect on ¹⁴C ages.

Isostatic rebound was likely accompanied by sea-level rise from the melting ice. Changes in water loads during the glacial cycle may have also had a crustal response such that oceanic crustal uplift occurred during glaciation when large volumes of water were locked up in the ice sheet. During deglaciation, this water would have been released resulting in the re-depression of the oceanic crust (Benn and Evans, 1998). Kotteff et al. (1993) recognized evidence for rapid sea-level rise prior to the onset of postglacial uplift along the coast of southern Maine. Sea-level rise would destroy delta surfaces and keep the deltas submerged longer, again, providing younger exposure ages.

Finally, erosion of the topsets would also effect TCN ages. An erosion rate of 0.035 mm/yr (or 52 cm in 15 ka) can contribute to explaining the disparity between the TCN ages and the ¹⁴C ages. This amount may be reasonable, on the order of the uncertainty in the amount of sediment that has been eroded from the topsets since the Holocene.

How can ¹⁴C ages be too old?	How can TCN ages be too young?
1. location with respect to delta	1. delayed emergence (smaller effect as marine limit is approached)
2. reservoir effect underestimated for marine ages	2. erosion (max)
3. "old" carbon contamination on terrestrial ages in marine sediments.	3. snow, eolian, tree cover
	4. inheritance over-corrected
	5. density too low
	6. production rate over-estimated

Table 5.2. Factors that may explain the difference between the ¹⁴C and TCN ages.

6 Conclusions

The ^{10}Be concentrations in the Auburn Plains delta profile show a good fit to the theoretical curve of exponential decrease in concentration with depth and demonstrates that TCN dating can precisely date deltaic sediment. In contrast, the ^{10}Be concentrations in the Dayton delta and Jailhouse delta profiles do not follow the expected pattern of decreased concentration with depth. The profile method was useful in identifying trouble profiles and non-behaved samples which led to the reanalysis of two samples from both deltas.

Inheritance becomes an important factor in trying to exposure date deltaic sediment as seen in the inheritance corrections applied to the samples from Auburn Plains delta. Given the problematic depth profiles from the Dayton and Jailhouse delta samples and from the inheritance corrections applied to the Auburn Plains delta samples, the profile method is considered to be necessary to date deltaic sediment. However, fewer samples can be required if two samples, one in the subsurface below the mixing zone and one at depth, are obtained similar to the technique employed by Anderson et al. (1996).

The exposure age of Auburn Plains Delta, after all adjustments were made, is 11.0 ± 0.9 ka. This age TCN dating can be used without other forms of dating providing that a depth profile method is employed. The depth profile method also allowed the amount of inheritance (1.46×10^4 atom g^{-1}) in Auburn Plains delta to be estimated. The sensitivity analysis confirmed that reasonable values for density were used and showed the effects of erosion on the TCN ages. The profile method was again beneficial in allowing potential erosion rates to be calculated. The sensitivity analysis also provides insight for sampling

strategies on other raised deltas and interpretations of exposure ages of deltas.

Future work

Having exposure ages in southern Maine is important because it tells us more about the retreat and dynamics of the LIS, particularly the timing and nature of post-glacial uplift as well as the timing of relative sea-level change since deglaciation.

However, more TCN dates are required to determine whether other deltas in southern Maine can be added to or constrain existing records of crustal unloading and rebound. This region has over 100 glaciomarine deltas, many adjacent to the marine limit, that would be suitable for the TCN technique.

Careful sampling strategy is essential. One additional sampling consideration should be applied to any dates obtained in deltas located below the marine limit. Any dates in these regions must consider submergence (and lower TCN production rates). The obtained TCN ages would be younger towards the coast to reflect the time it took for the shift between transgression and regression. These deltas would have taken longer to emerge resulting in younger TCN ages. Wave reworking would result in erosion of delta surfaces, again resulting in younger TCN ages.

Having exposure ages on deltas is important because they typically have little radiocarbon dateable material in them and must rely on radiocarbon ages obtained from the closest dateable material. TCN dating of deltas may be a significant development in the chronology of deglacial histories and relative sea-level histories of coastal glaciated regions.

References

- Anderson, R.S. Repka, J.L., and Dick, G.S. 1996. Explicit treatment of inheritance in dating depositional surfaces using in situ ^{10}Be and ^{26}Al , *Geology*, **24**, no.1, p. 47-51.
- Barnhardt, W.A., Gehrels, W.R., Belknap, D.F., and Kelley J.T. 1995. Late Quaternary relative sea-level change in the western Gulf of Maine: Evidence for a migrating glacial forebulge, *Geology*, **23**, no.4, p. 317-320.
- Benn D., and Evans, D.J. 1998. *Glaciers and Glaciation*. Arnold, London, U.K.
- Borns, H.W. Jr., Doner, L.A., Dorion, C.C., Jacobson, G.L. Jr., Kaplan, M.R., Kreutz, K.J., Lowell, T.V., Thompson, W.B., and Weddle, T.K. 2004. The deglaciation of Maine, U.S.A. In: Ehlers, J. and Gibbard, P.L. (eds.), *Quaternary Glaciations - Extent and Chronology, Part 2*: Elsevier B.V., p.89-109.
- Dorion, C.C., Balco, G.A., Kaplan, M.R., Kreutz, K.J., Wright, J.D. & Borns, H.W. Jr. 2001. Stratigraphy, palaeoceanography, chronology and environment during deglaciation of Eastern Maine. In: Weddle, T.K. & Retelle, M.J. (eds), *Deglacial history and relative sea-level changes, northern New England and adjacent Canada*. Geological Society of America, Special Paper, **351**, p. 215-242.
- Gosse, J.C. and Stone, J.O. 2001. Terrestrial cosmogenic nuclide methods passing milestones toward paleo-altimetry. *Eos, Transactions, American Geophysical Union*, **82**, no.7, p. 82, 86, 89.
- Gosse, J.C. and Phillips, F.M. 2001. Terrestrial Cosmogenic nuclides: theory and application. *Quaternary Science Review*, **20**, 1475-1560.
- Gosse, J.C. 1994. *Surficial Geology of the Standish 7.5 minute Quadrangle, York and Cumberland Counties, Maine*. Open File 94-10. Maine Geological Survey.
- Hancock, G.S., Anderson, R.S., Chadwick, O.A., and Finkel, R.C. 1999. Dating fluvial terraces with ^{10}Be and ^{26}Al profiles: application to the Wind River, Wyoming, *Geomorphology*, **27**, p.41-60.
- Hilchey, A. 2004. *Holocene Deglacial Geologic History of the Ravn River Valley, Northern Baffin Island, Nunavut*. Honours thesis: Dalhousie University, 134p.
- Hunter, L.E. 1990. *Surficial Geology of the Bar Mills Quadrangle, York County, Maine*. Open File 90-34. Maine Geological Survey.

- Koteff, C., Robinson, G.R., Goldsmith, R., and Thompson, W. 1993. Delayed postglacial uplift and synglacial sea levels in coastal central New England: Quaternary Research, **40**, p.46-54.
- Koteff, C. and Larsen (1989). Postglacial uplift in western New England: Geologic evidence for delayed rebound. In: Gregersen, S. and Basham, P.W.(eds), Earthquakes at North Atlantic Passive margins: Neotectonics and Postglacial Rebound, p.105-123. Kluwer Academic, Amsterdam.
- Koteff, C., and Pessl, F.J. (1981). Systematic Ice Retreat in New England: U.S. Geological Survey, Professional Paper 1179, 20p.
- Lal, D.1988. In situ-produced cosmogenic isotopes in terrestrial rocks. Annual review of Earth and Planetary Sciences, **16**, 355-388.
- Lowell, T.V. (1985). Late Wisconsin ice flow reversal and deglaciation, northwestern Maine, in Borns, H.W., Jr., LaSalee, P. and Thompson, W.B. (eds.), Late Pleistocene history of Northeastern New England and adjacent Quebec. Geological Society of America, Special Paper, **197**, 71-83.
- Peltier, W.R. 1998. Postglacial variations in the level of the sea: Implications for climate dynamics and solid-Earth geophysics: Review of geophysics, **36**, no. 4, p 603-689.
- Smart, D.F., and Shea, M.A. (Ed.), 1985. Galactic cosmic radiation and solar energetic particles. Handbook of Geophysics and the Space Environment. Air Force Geophysics Laboratory, 6-1-6, 29 pp.
- Smith, G.W., 1985. Chronology of Late Wisconsinan deglaciation of Coastal Maine. In Borns, H.W., Jr., LaSalee, P. and Thompson, W.B. (eds.), Late Pleistocene history of Northeastern New England and adjacent Quebec. Geological Society of America, Special Paper, **197**, 29-44.
- Stuiver, M. and Borns, H.W. Jr., 1975. Late Quaternary marine invasion in Maine: its chronology and associated crustal movement: Geological Society of America, Bulletin, **86**, p.99-104.
- Retelle, M.J. & Weddle, T.K. 2001. Deglaciation and relative seal level chronology, Casco Lowland and lower Androscoggin River Valley, Maine. In: Weddle, T.K. & Retelle, M.J. (eds), Deglacial history and relative sea-level changes, northern New England and adjacent Canada. Geological Society of America, Special Paper, **351**, 191-214.

- Ridge, J.C., Canwell, B.A., Kelly, M.A. & Kelley, S.Z. 2001. An atmospheric ^{14}C chronology for Late Wisconsinan deglaciation and sea-level change in eastern New England using varve and paleomagnetic records. In Weddle, T.K. & Retelle, M.J. (eds), Deglacial history and relative sea-level changes, northern New England and adjacent Canada. Geological Society of America, Special Paper, **351**, 171-189.
- Thompson, W. B. 1982. Recession of the Late Wisconsinan Ice Sheet in Coastal Maine. In Larson, G.J., and Stone, B.D. (eds.), Late Wisconsin glaciation of New England: Kendall/Hunt, Dubuque, Iowa, p.211-228.
- Thompson, W.B., and Borns, H.W. Jr., 1985b, Surficial geologic map of Maine: Maine Geological Survey, scale 1:500,000.
- Thompson, W.B., Crossen, K.J., Borns, H.J., Jr., and Anderson, B.G. 1989. Glaciomarine deltas of Maine and their relation to Late Pleistocene-Holocene crustal movements, in Anderson, W.A., and Borns, H.W., Jr. (eds), Neotectonics of Maine: studies in seismicity, crustal warping, and sea-level change: Maine Geological Survey, p.43-67.
- Thompson, W., Fowler, B.K., and Dorion, C.C. 1999. Deglaciation of the northwest White Mountains, New Hampshire: *Geographie Physique et Quaternaire*, **53**, no.1, p.59-79.
- Thompson, W.B. 2001. Deglaciation of Western Maine. In Weddle, T.K. & Retelle, M.J. (eds), Deglacial history and relative sea-level changes, northern New England and adjacent Canada. Geological Society of America, Special Paper, **351**, 109-123.

Appendix 1 Chemistry Data

WS4_QtzDissolution

This worksheet outlines the steps for dissolving quartz and adding Be carrier.

Chemist: ^{JG/GY}

Date: ^{form:mm/dd/yy}

	1	2	3	4	5	6	7	8	examples
CNEF ID	1236	1237	1238	1239	1240	1241	1223	1504	105
Sample ID	ME-02-JHD-109	ME-02-JHD-110	ME-02-DAY-112	ME-02-DAY-113	ME-02-DAY-114	ME-02-DAY-115	KBC-02-33	Blank	WY-96-001
300 ml vessel ID	B1	B2	B3	B4	B5	B6	B7	B8	AA
Beryl Carrier ID									Bel-Carrier
	(tare balance after each measurement)								
Mass 300 ml vessel	150.2751	150.3024	150.3055	150.2800	150.4460	150.2886	150.2979	150.2216	148.7188 g
Mass 40g quartz	42.6200	56.1797	31.7297	18.3455	56.0139	56.2110	56.2625	0.0000	20.0000 g
Mass Be carrier	0.2798	0.3009	0.3048	0.3058	0.2981	0.3046	0.3050	0.3092	1.0147 g

SAVE AS: C:/Chemistry/CHEM_WK YYYYMMDD .xls then PRINT

- Add 20 ml conc. HF and 2 ml HClO₄ per 5 g of quartz
- Add 5 ml Aqua Regia
- Heat at 100-125° C until quartz dissolves, add HF if needed
- Raise to 200° C and evaporate to dryness
- Add 5 ml HClO₄ and evaporate to dryness
- Add 8 to 10 ml conc. HNO₃, swirl, and evaporate to dryness
- Dissolved dried sample in 20 ml of 2% HNO₃.

Comments

Sept 9: balance calibration before use
add 6mL HClO₄, use H₂O to rinse side wall, dry at 200C

Sept 12: Add HNO₃ 10 ML 100C

WS5_ICP Aliquot and Al spiking

This worksheet outlines the steps for collecting ICP aliquots and adding Al carrier.

Chemist: ^{GY}

Date: ^{form: 02/17/01}

- 1 Label one 10 ml volumetric flasks per sample (8)
- 2 Label one ICP vial with CNEF ID per sample (8)

	1	2	3	4	5	6	7	8	examples
CNEF ID	1236	1237	1238	1239	1240	1241	1223	1504	105
Sample ID	ME-02-RD-109	ME-02-RD-110	ME-02-DAY-112	ME-02-DAY-113	ME-02-DAY-114	ME-02-DAY-115	KBC-02-33	Blank	WY-96-001
Al carrier ID								Al Carrier	ALI-carrier
Quant-EM est. Al in qtz									ppm
Volume carrier to add to smpl								1.0061	ml
Volume carrier to add to vol A									ml
Volume carrier to add to vol. B									ml
Tare between mass measurements									
Mass 100 ml volumetric	67.6868	66.8414	68.2937	69.2261	67.7940	67.0057	68.8733	67.1810	66.9239 g
100ml volumetric+sample+2%HCl	168.7455	168.0560	169.3143	170.0188	168.9955	168.2144	169.7480	168.1090	166.9875 g
Mass 5 ml smpl pipetted to vol A	10.0547	10.1093	10.0911	10.0883	10.1114	10.1000	10.0647	10.0534	5.0000 g
Final Mass of 100 ml vol and smpl	158.6873	157.9416	159.2203	159.9260	158.8809	158.1099	159.6797	158.0507	1.0100 g
Mass Al carrier to remaining (row18)									1.0100 g
10ml Vol Weight	42.0168	40.7563	40.8499	40.8188	40.8123	41.2325	40.9099	40.9512	
Unaccounted mass									0.0100 g

PRINT this form

Get digestion vessel and cover ready, Do not wipe now.

Transfer the 90 ml sample back into vessel

Bring contents of volumetrics A and B to 10 ml

Transfer contents volumetrics to ICP vials with same number

GY July 16, 2003 update

WS6_Anion Column Chemistry

This worksheet outlines the steps for the Anion Column Chemistry

Chemist: ^{GY}

Date: ^{form: MM/DD/YY}

Print this page

Evaporate 80 ml to dryness at 100-120°C (will take at least 3 hrs)

Dissolve in 10 ml 9N HCl (let stand for several hours)

Transfer to 15 ml centrifuge tubes, rinse digestion vessels with 9N HCl to bring volume in tube to 10 ml

Centrifuge at 1500 rpm or higher for minimum of 10 minutes

Allow any 9 N HCl in columns to drain out; discard

Column ID	A	B	C	D	E	F	G	H	AnionColumnID
CNEF ID	1236	1237	1238	1239	1240	1241	1223	1504	105
Sample ID	E-02-JHD-	E-02-JHD-	E-02-DAY-	E-02-DAY-	E-02-DAY-	E-02-DAY-	KBC-02-33	Blank	WY-96-001

With stopcock closed, pipet sample (avoid residue) onto columns.

Collect sample in same (wiped) 120 ml teflon vessel

Elute with 30 ml 9 N HCl, and collect that, close stopcock

5 ml 4.5 N HCl, collect Anion Supernate in labeled 100 ml bottle

100 ml 1 N HCl, collect Anion Supernate

50 ml deionized water. Discard.

CONDITION ANION COLUMN

(bottle A1) 50 ml 1N HCl, discard

(bottle A2) 50 ml 4.5 N HCl, discard

(bottle A3) 100 ml 9 N HCl, discard, but retain acid approx. 2 mm above resin

Comments

everything is fine
vessels are on hotplate to dry @ 120C

WS8_Cation Column Chemistry

This worksheet outlines the steps for the Cation Column Chemistry

Chemist: ^{GY/JG}

Date: ^{mm/dd/yy}

Print this page

- 1 Dissolve in 5 ml conc. HCl and evaporate to dryness at 125°C
- 2 Redissolve in 2.5 ml 1N HCl and 2.5 ml 0.5 N HCl
- 3 Transfer to centrifuge tube, rinse with 1 ml 0.5N, and centrifuge

Column ID	1	2	3	4	5	6	7	8	examples
CNEF ID	1236	1237	1238	1239	1240	1241	1223	1504	105
Sample ID	E-02-JHD-1	E-02-JHD-1	E-02-DAY-1	E-02-DAY-1	E-02-DAY-1	E-02-DAY-1	KBC-02-33	Blank	WY-96-001

- 4 Pipette all of the sample into designated conditioned cation column
- 5 Discard the eluant. Add 220 ml 0.5 N HCL (bottle C6)
- 6 Collect eluant as Cation Supernate, add 200 ml 0.5 N HCl (bottle C7)
- 7 Collect eluant as Be-Sample into vessels.
- 8 Add 30 ml 1N HCl (bottle8)
- 9 Save this as Be-sample as well.
- 10 Add 100 ml 4.5 N HCl, save as Al sample.
- 11
- 12
- 13 **CONDITION CATION COLUMN**

- (bottle C1) 100 ml 9N HCl
- (bottle C2) 50 ml 4.5 N HCl
- (bottle C3) 50 ml 1 N HCl
- (bottle C4) 50 ml water
- (bottle C5) 100 ml 0.5 N HCl

WS9_Be Sample Chemistry

This worksheet outlines the steps to prepare the BeO sample

Chemist: ^{GY}

Date: ^{form: mm/dd/yy}

Print this page

- 1 Evaporate Be Sample from column in wiped digestion vessels at 125°C
- 2 Add 2-5 ml 20% perchloric and evaporate at 200°C
- 3 Again, add 2-5 ml 20% perchloric and evaporate at 200°C
- 4 Dissolve sample in 10 ml of 0.5 N HCl (optima grade)
- 5 Transfer to 15 ml centrifuge tube
- 6 Centrifuge and decant into clean centrifuge tube
- 7 Heat centrifuge tubes in water bath at 60°C
- 8 Precipitate Be(OH)₂ using Matheson ultimate grade ammonia gas
Gently bubble NH₃ with clean pipet tip on hose
for ca.15 bubbles, or ca. 8-12 sec until ppt forms
Optimum pH=9.2; 1N HCl may be added
- 9 Centrifuge 15 min., decant (save and redo 8 if pH of liquid is < 8)
- 10 Wash with water, vortex, centrifuge for 10 min, and decant
- 11 Record mass quartz vials, label, and place them in furnace holder

CNEF ID	1236	1237	1238	1239	1240	1241	1223	1504	105
Sample ID	E-02-JHD-	E-02-JHD-	E-02-DAY-	E-02-DAY-	E-02-DAY-	E-02-DAY-	KBC-02-33	Blank	WY-96-001
Mass Qtz Vial	2.5431	2.3651	2.4374	2.4644	2.4188	2.5755	2.4778	2.4895	2.1400 g
Mass Vial+Spl	2.5446	2.3665	2.4391	2.4657	2.42	2.5773	2.4791	2.49	2.1410 g
Mass Spl	0.0015	0.0014	0.0017	0.0013	0.0012	0.0018	0.0013	0.0005	1 mg

- 12 Add 1 small drop of water with micropipet, slurry precipitate
- 13 Transfer sample into quartz vial, cover with alumina vial
- 14 Heat in oven at 120°C for 2-3 hours
- 15 Let cool and scrape sample down from walls of quartz tube
- 18 Place in furnace. Convert to BeO in furnace at 850°C for minimum 1 hr
- 19 Determine mass of vial + sample

WS10_AI Sample Chemistry

This worksheet outlines the steps to prepare the Al oxide sample

Chemist: ^{GY}

Date: ^{form: mm/dd/yy}

Print this page

- 1 Evaporate Al Sample from column in wiped teflon vessel at 125°C
- 2 Dissolve sample in 10 ml of 0.5 N HCl (optima grade)
- 3 Transfer to 15 ml centrifuge tube
- 4 Centrifuge and decant into clean centrifuge tube
- 5 Heat centrifuge tubes in water bath at 60°C
- 6 Precipitate Al(OH)₃ using 50% NH₃OH (drops: 25, 5, 5, 3, 2...)

Optimum pH=6.3; 1N HCl may be added

- 7 Centrifuge 15 min., decant (save and redo 6 if pH of liquid is < 8)
- 8 Wash with water, vortex, centrifuge for 10 min, and decant
- 9 Record mass quartz vials, label, and place them in furnace holder

CNEF ID	1236	1237	1238	1239	1240	1241	1223	1504	105
Sample ID	E-02-JHD-1	E-02-JHD-1	E-02-DAY-1	E-02-DAY-1	E-02-DAY-1	E-02-DAY-1	KBC-02-33	Blank	WY-96-001
Mass Qtz Vial									2.1400 g
Mass Vial+Spl									2.1410 g
Mass Spl	0	0	0	0	0	0	0	0	1 mg

- 10 Add 1 small drop of water with micropipet, slurry precipitate
- 11 Transfer sample into quartz vial, cover with alumina vial
- 12 Heat in oven at 120°C for 2-3 hours
- 13 Let cool and scrape sample down from walls of quartz tube
- 14 Convert to Al₂O₃ in furnace at 950°C for minimum of 1 hr
- 15 Determine mass of vial + sample

WS4_QtzDissolution

This worksheet outlines the steps for dissolving quartz and adding Be carrier.

Chemist: ^{JG/GY}

Date: ^{form:mm/dd/yy}

	1	2	3	4	5	6	7	8	examples
CNEF ID	1229	1230	1231	1232	1233	1224	1225	1530	105
Sample ID	ME-02-APD-101	ME-02-APD-102	ME-02-APD-103	ME-02-APD-104	ME-02-APD-105	MC02-1	MC02-2	Blank	WY-96-001
300 ml vessel ID	B1	B2	B3	B4	B5	B6	B7	B8	AA
Beryl Carrier ID	Be-3 bottle 4	Be-3 bottle 4	Be-3 bottle 4	Be-3 bottle 4	Be-3 bottle 4	Be-3 bottle 4	Be-3 bottle 4	Be-3 bottle 4	BeI-Carrier
	(tare balance after each measurement)								
Mass 300 ml vessel	150.3085	150.3019	150.3093	150.2789	150.4461	150.2945	150.3020	150.2236	148.7188 g
Mass 40g quartz	28.6987	50.0644	24.0665	49.9885	38.8819	50.4722	50.1808	0.0000	20.0000 g
Mass Be carrier	0.2964	0.3033	0.2966	0.3129	0.3033	0.3031	0.3050	0.2982	1.0147 g

SAVE AS: C:/Chemistry/CHEM_WK YYMMDD .xls then PRINT

- 1 Add 20 ml conc. HF and 2 ml HClO₄ per 5 g of quartz
- 2 Add 5 ml Aqua Regia
- 3 Heat at 100-125° C until quartz dissolves, add HF if needed
- 4 Raise to 200° C and evaporate to dryness
- 5 Add 5 ml HClO₄ and evaporate to dryness
- 6 Add 8 to 10 ml conc. HNO₃, swirl, and evaporate to dryness
- 7 Dissolved dried sample in 20 ml of 2% HNO₃.

Comments

Oct 6: Add 25mL HF and 15mL HNO3 to
Oct 7: start to dry

WS5_ICP Aliquot and Al spiking

This worksheet outlines the steps for collecting ICP aliquots and adding Al carrier.

Chemist: ^{DB}

Date: ^{form: 02/17/01}

- 1 Label one 10 ml volumetric flasks per sample (8)
- 2 Label one ICP vial with CNEF ID per sample (8)

	1	2	3	4	5	6	7	8	examples
CNEF ID	1229	1230	1231	1232	1233	1224	1225	1530	105
Sample ID	ME-02-APD-101	ME-02-APD-102	ME-02-APD-103	ME-02-APD-104	ME-02-APD-105	MC02-1	MC02-2	Blank	WY-96-001
Al carrier ID							Al carrier4(Jan 16, 2001)		ALI-carrier
Quant-EM est. Al in qtz								0	ppm
Volume carrier to add to smpl								1.0176	ml
Volume carrier to add to vol A									ml
Volume carrier to add to vol. B									ml
Tare between mass measurements									
Mass 100 ml volumetric	67.4180	67.3569	68.8736	66.7112	67.7442	65.2043	67.7314	67.6901	66.9239 g
100ml volumetric+sample+2%HCl	168.5085	168.3753	169.6853	167.6535	168.7345	166.3411	169.0044	169.5598	166.9875 g
Mass 5 ml smpl pipetted to vol A	10.0877	10.0877	10.0620	10.0941	10.0656	10.0914	10.0120	10.1407	5.0000 g
Final Mass of 100 ml vol and smpl	158.4102	158.2806	159.6187	157.5421	158.6646	156.2460	158.8809	159.4055	1.0100 g
Mass Al carrier to remaining (row18)									1.0100 g
10ml Vol mass									
Unaccounted mass									0.0100 g

PRINT this form

- 3 Get digestion vessel and cover ready, Do not wipe now.
- 4 Transfer the 90 ml sample back into vessel
- 5 Bring contents of volumetrics A and B to 10 ml
- 6 Transfer contents volumetrics to ICP vials with same number

GY July 16, 2003 update

WS6_Anion Column Chemistry

This worksheet outlines the steps for the Anion Column Chemistry

Chemist: ^{DB}

Date: ^{form: MM/DD/YY}

Print this page

- 1 Evaporate 80 ml to dryness at 100-120°C (will take at least 3 hrs)
- 2 Dissolve in 10 ml 9N HCl (let stand for several hours)
- 3 Transfer to 15 ml centrifuge tubes, rinse digestion vessels with 9N HCl to bring volume in tube to 10 ml
- 4 Centrifuge at 1500 rpm or higher for minimum of 10 minutes
- 5 Allow any 9 N HCl in columns to drain out; discard

Column ID	A	B	C	D	E	F	G	H	AnionColumnID
CNEF ID	1229	1230	1231	1232	1233	1224	1225	1530	105
Sample ID	ME-02-APD-101	ME-02-APD-102	ME-02-APD-103	ME-02-APD-104	ME-02-APD-105	MC02-1	MC02-2	Blank	WY-96-001

- 6 With stopcock closed, pipet sample (avoid residue) onto columns.
- 7 Collect sample in same (wiped) 120 ml teflon vessel
- 8 Elute with 30 ml 9 N HCl, and collect that, close stopcock
- 9 5 ml 4.5 N HCl, collect Anion Supernate in labeled 100 ml bottle
- 10 100 ml 1 N HCl, collect Anion Supernate
- 11 50 ml deionized water. Discard.
- 12 **CONDITION ANION COLUMN**

(bottle A1) 50 ml 1N HCl, discard
 (bottle A2) 50 ml 4.5 N HCl, discard
 (bottle A3) 100 ml 9 N HCl, discard, but retain acid approx. 2 mm above resin

Comments

1224, 1225 are dark yellow, the rest are regular yellow colour, blank is clear

WS7_Controlled Precipitate

This worksheet outlines the steps for the controlled precipitation chemistry

Chemist: ^{DB} GY

Date: ^{form: MM/DD/YY} 10/28/04

Print this page

- 1 Evaporate "anion" elute to dryness at 125°C
- 2 Dissolve in 10 ml of a 1:1 solution of 0.5N HCl and 2% NH₄Cl
- 3 Transfer to 15 ml centrifuge, centrifuge for 10 minutes
- 4 Decant into clean test tube, heat in water bath at 60°C
- 5 Add drops of 1:1 NH₄OH:H₂O to pH=9.2 (5 drops first then single)
- 6 Centrifuge for 15 minutes
- 7 Check pH of liquid, if less than pH=7, redo step 5
- 8 Decant, save with Anion Supernate
- 9 Wash with deionized water, vortex, centrifuge, decant
- 10 Wash with deionized water, vortex, centrifuge, decant
- 11 Wash with deionized water, vortex, centrifuge, decant

CNEF ID	1229	1230	1231	1232	1233	1224	1225	1530	#
Sample ID	ME-02-APD-101	ME-02-APD-102	ME-02-APD-103	ME-02-APD-104	ME-02-APD-105	MC02-1	MC02-2	Blank	
Approx. vol. Ptte	0.8	1.2	1	1	1.2	0.8	0.7	0.3	

Comments

1225 and 1530 looks like gelish, little brown color. The rest of sample are all white color. "cloudy white".

WS8_Cation Column Chemistry

This worksheet outlines the steps for the Cation Column Chemistry

Chemist: ^{DB}

Date: ^{mm/dd/yy}

Print this page

- 1 Dissolve in 5 ml conc. HCl and evaporate to dryness at 125°C
- 2 Redissolve in 2.5 ml 1N HCl and 2.5 ml 0.5 N HCl
- 3 Transfer to centrifuge tube, rinse with 1 ml 0.5N, and centrifuge

Column ID	1	2	3	4	5	6	7	8	examples
CNEF ID	1229	1230	1231	1232	1233	1224	1225	1530	105
Sample ID	E-02-APD-1	E-02-APD-1	E-02-APD-1	E-02-APD-1	E-02-APD-1	MC02-1	MC02-2	Blank	WY-96-001

- 4 Pipette all of the sample into designated conditioned cation column
- 5 Discard the eluant. Add 220 ml 0.5 N HCL (bottle C6)
- 6 Collect eluant as Cation Supernate, add 200 ml 0.5 N HCl (bottle C7)
- 7 Collect eluant as Be-Sample into vessels.
- 8 Add 30 ml 1N HCl (bottle8)
- 9 Save this as Be-sample as well.
- 10 Add 100 ml 4.5 N HCl, save as Al sample.
- 11
- 12
- 13 **CONDITION CATION COLUMN**

(bottle C1) 100 ml 9N HCl
 (bottle C2) 50 ml 4.5 N HCl
 (bottle C3) 50 ml 1 N HCl
 (bottle C4) 50 ml water
 (bottle C5) 100 ml 0.5 N HCl

WS9_Be Sample Chemistry

This worksheet outlines the steps to prepare the BeO sample

Chemist: ^{DB}

Date: ^{form: mm/dd/yy}

Print this page

- 1 Evaporate Be Sample from column in wiped digestion vessels at 125°C
- 2 Add 2-5 ml 20% perchloric and evaporate at 200°C
- 3 Again, add 2-5 ml 20% perchloric and evaporate at 200°C
- 4 Dissolve sample in 10 ml of 0.5 N HCl (optima grade)
- 5 Transfer to 15 ml centrifuge tube
- 6 Centrifuge and decant into clean centrifuge tube
- 7 Heat centrifuge tubes in water bath at 60°C
- 8 Precipitate Be(OH)₂ using Matheson ultimate grade ammonia gas
 - Gently bubble NH₃ with clean pipet tip on hose
 - for ca. 15 bubbles, or ca. 8-12 sec until ppt forms
 - Optimum pH=9.2; 1N HCl may be added
- 9 Centrifuge 15 min., decant (save and redo 8 if pH of liquid is < 8)
- 10 Wash with water, vortex, centrifuge for 10 min, and decant
- 11 Record mass quartz vials, label, and place them in furnace holder

CNEF ID	1229	1230	1231	1232	1233	1224	1225	1530	
Sample ID	-02-APD-	-02-APD-	-02-APD-	-02-APD-	-02-APD-	MC02-1	MC02-2	Blank	¹⁰⁵
Mass Qtz Vial	2.4299	2.5246	2.4324	2.4233	2.491	2.3336	2.4278	2.4918	^{WY-96-001} 2.1400 g
Mass Vial+Spl	2.431	2.5254	2.433	2.4248	2.4918	2.4918	2.4289	2.4926	2.1410 g
Mass Spl	0.0011	0.0008	0.0006	0.0015	0.0008	0.1582	0.0011	0.0008	1 mg

- 12 Add 1 small drop of water with micropipet, slurry precipitate
- 13 Transfer sample into quartz vial, cover with alumina vial
- 14 Heat in oven at 120°C for 2-3 hours
- 15 Let cool and scrape sample down from walls of quartz tube
- 18 Place in furnace. Convert to BeO in furnace at 850°C for minimum 1 hr
- 19 Determine mass of vial + sample

WS10_AI Sample Chemistry

This worksheet outlines the steps to prepare the Al oxide sample

Chemist: ^{DB}

Date: ^{form: mm/dd/yy}

Print this page

- ₁ Evaporate Al Sample from column in wiped teflon vessel at 125°C
- ₂ Dissolve sample in 10 ml of 0.5 N HCl (optima grade)
- ₃ Transfer to 15 ml centrifuge tube
- ₄ Centrifuge and decant into clean centrifuge tube
- ₅ Heat centrifuge tubes in water bath at 60°C
- ₆ Precipitate Al(OH)₃ using 50% NH₃OH (drops: 25, 5, 5, 3, 2...)

Optimum pH=6.3; 1N HCl may be added

- ₇ Centrifuge 15 min., decant (save and redo ₆ if pH of liquid is < 8)
- ₈ Wash with water, vortex, centrifuge for 10 min, and decant
- ₉ Record mass quartz vials, label, and place them in furnace holder

CNEF ID	1229	1230	1231	1232	1233	1224	1225	1530	105
Sample ID	E-02-APD-	E-02-APD-	E-02-APD-	E-02-APD-	E-02-APD-1	MC02-1	MC02-2	Blank	WY-96-001
Mass Qtz Vial									2.1400 g
Mass Vial+Spl									2.1410 g
Mass Spl	0	0	0	0	0	0	0	0	1 mg

- ₁₀ Add 1 small drop of water with micropipet, slurry precipitate
- ₁₁ Transfer sample into quartz vial, cover with alumina vial
- ₁₂ Heat in oven at 120°C for 2-3 hours
- ₁₃ Let cool and scrape sample down from walls of quartz tube
- ₁₄ Convert to Al₂O₃ in furnace at 950°C for minimum of 1 hr
- ₁₅ Determine mass of vial + sample

WS4_QtzDissolution

This worksheet outlines the steps for dissolving quartz and adding Be carrier.

Chemist: ^{JG/GY}

Date: ^{form:mm/dd/yy}

	1	2	3	4	5	6	7	8	examples
CNEF ID	1237	1241	1337	1338	1227	1228	1216	1536	105
Sample ID	ME-02-PHD-110	ME-02-DAY-115	ORE-01-McG-05	VAN-01-MYRA-06	MC-02-4	MC-02-5	K02-229-35	Blank	WY-96-001
300 ml vessel ID	B15	B18	B19	B20	B21	B22	B23	B24	AA
Beryl Carrier ID									Bel-Carrier
	(tare balance after each measurement)								
Mass 300 ml vessel	150.2943	150.2565	150.2917	150.3167	155.2591	150.3481	150.4513	150.3191	148.7188 g
Mass 40g quartz	55.1719	41.2430	26.2997	55.1408	50.3518	55.0910	18.2683	0.0000	20.0000 g
Mass Be carrier	0.3029	0.3090	0.3013	0.3143	0.2958	0.2992	0.2995	0.3057	1.0147 g

SAVE AS: C:/Chemistry/CHEM_WK YYYYMMDD .xls **then PRINT**

- 1 Add 20 ml conc. HF and 2 ml HClO₄ per 5 g of quartz
- 2 Add 5 ml Aqua Regia
- 3 Heat at 100-125° C until quartz dissolves, add HF if needed
- 4 Raise to 200° C and evaporate to dryness
- 5 Add 5 ml HClO₄ and evaporate to dryness
- 6 Add 8 to 10 ml conc. HNO₃, swirl, and evaporate to dryness
- 7 Dissolved dried sample in 20 ml of 2% HNO₃.

Comments

WS5_ICP Aliquot and AI spiking

This worksheet outlines the steps for collecting ICP aliquots and adding AI carrier.

Chemist: ^{GY}

Date: ^{form: 02/17/01}

- 1 Label one 10 ml volumetric flasks per sample (8)
- 2 Label one ICP vial with CNEF ID per sample (8)

	1	2	3	4	5	6	7	8	examples
CNEF ID	1237	1241	1337	1338	1227	1228	1216	1536	105
Sample ID	ME-02-PHD-110	ME-02-DAY-115	ORE-01-McG-05	VAN-01-MYRA-06	MC-02-4	MC-02-5	K02-229-35	Blank	WY-96-001
AI carrier ID								AI Carrier4	ALI-carrier
Quant-EM est. AI in qtz								0	ppm
Volume carrier to add to smpl								1.0087	ml
Volume carrier to add to vol A									ml
Volume carrier to add to vol. B									ml
Tare between mass measurements									
Mass 100 ml volumetric	67.1373	66.7123	67.1826	66.4907	68.2943	67.7320	66.9340	65.2043	66.9239 g
100ml volumetric+sample+2%HCl	168.1930	167.8926	168.2338	167.4841	170.5724	168.8665	168.0288	166.3302	166.9875 g
Mass 5 ml smpl pipetted to vol A	10.0161	10.0078	10.0011	10.0143	10.0879	10.0252	10.0040	10.0142	5.0000 g
Final Mass of 100 ml vol and smpl	158.1734	157.8778	158.2280	157.4662	160.4786	158.8373	158.0205	156.2988	1.0100 g
Mass AI carrier to remaining (row18)									1.0100 g
Unaccounted mass									0.0100 g

PRINT this form

- 3 Get digestion vessel and cover ready, Do not wipe now.
- 4 Transfer the 90 ml sample back into vessel
- 5 Bring contents of volumetrics A and B to 10 ml
- 6 Transfer contents volumetrics to ICP vials with same number

GY July 16, 2003 update

WS6_Anion Column Chemistry

This worksheet outlines the steps for the Anion Column Chemistry

Chemist: GY^{GY}

Date: 01/26/05^{form: MM/DD/YY}

Print this page

- 1 Evaporate 80 ml to dryness at 100-120°C (will take at least 3 hrs)
- 2 Dissolve in 10 ml 9N HCl (let stand for several hours)
- 3 Transfer to 15 ml centrifuge tubes, rinse digestion vessels with 9N HCl to bring volume in tube to 10 ml
- 4 Centrifuge at 1500 rpm or higher for minimum of 10 minutes
- 5 Allow any 9 N HCl in columns to drain out; discard

Column ID	A	B	C	D	E	F	G	H	AnionColumnID
CNEF ID	1237	1241	1337	1338	1227	1228	1216	1536	105
Sample ID	-02-PHD-	-02-DAY-	E-01-McG	I-01-MYR	MC-02-4	MC-02-5	K02-229-3	Blank	WY-96-001

- 6 With stopcock closed, pipet sample (avoid residue) onto columns.
- 7 Collect sample in same (wiped) 120 ml teflon vessel
- 8 Elute with 30 ml 9 N HCl, and collect that, close stopcock
- 9 5 ml 4.5 N HCl, collect Anion Supernate in labeled 100 ml bottle
- 10 100 ml 1 N HCl, collect Anion Supernate
- 11 50 ml deionized water. Discard.
- 12 **CONDITION ANION COLUMN**

(bottle A1) 50 ml 1N HCl, discard
 (bottle A2) 50 ml 4.5 N HCl, discard
 (bottle A3) 100 ml 9 N HCl, discard, but retain acid approx. 2 mm above resin

Comments

Anion columns used 4 times before this
 #7 column is new, previous one showing yellow colour
 1227 and 1228 are iron-rich, almost orange
 the rest are yellow (regular), blank is clear

WS7_Controlled Precipitate

This worksheet outlines the steps for the controlled precipitation chemistry

Chemist: GY^{GY}

Date: 01/31/05^{form: MM/DD/YY}

Print this page

- 1 Evaporate "anion" elute to dryness at 125°C
- 2 Dissolve in 10 ml of a 1:1 solution of 0.5N HCl and 2% NH₄Cl
- 3 Transfer to 15 ml centrifuge, centrifuge for 10 minutes
- 4 Decant into clean test tube, heat in water bath at 60°C
- 5 Add drops of 1:1 NH₄OH:H₂O to pH=9.2 (5 drops first then single)
- 6 Centrifuge for 15 minutes
- 7 Check pH of liquid, if less than pH=7, redo step 5
- 8 Decant, save with Anion Supernate
- 9 Wash with deionized water, vortex, centrifuge, decant
- 10 Wash with deionized water, vortex, centrifuge, decant
- 11 Wash with deionized water, vortex, centrifuge, decant

CNEF ID	1237	1241	1337	1338	1227	1228	1216	1536	#
Sample ID	ME-02-PHD-110	ME-02-DAY-115	CRE-01-McG-05	VAN-01-MYRA-06	MC-02-4	MC-02-5	K02-228-35	Blank	
Approx. vol. Ptte	2	0.5	0.8	0.8	0.7	1	0.3	0.2	

Comments

all precipitate are white, good gel shape, solutions clear

WS8_Cation Column Chemistry

This worksheet outlines the steps for the Cation Column Chemistry

Chemist: ^{GY/JG}

Date: ^{mm/dd/yy}

Print this page

- 1 Dissolve in 5 ml conc. HCl and evaporate to dryness at 125°C
- 2 Redissolve in 2.5 ml 1N HCl and 2.5 ml 0.5 N HCl
- 3 Transfer to centrifuge tube, rinse with 1 ml 0.5N, and centrifuge

Column ID	1	2	3	4	5	6	7	8	examples
CNEF ID	1237	1241	1337	1338	1227	1228	1216	1536	105
Sample ID	ME-02-PHD-110	ME-02-DAY-115	ORE-01-McG-05	VAN-01-MYRA-06	MC-02-4	MC-02-5	K02-229-35	Blank	WY-96-001

- 4 Pipette all of the sample into designated conditioned cation column
- 5 Discard the eluant. Add 220 ml 0.5 N HCL (bottle C6)
- 6 Collect eluant as Cation Supernate, add 200 ml 0.5 N HCl (bottle C7)
- 7 Collect eluant as Be-Sample into vessels.
- 8 Add 30 ml 1N HCl (bottle8)
- 9 Save this as Be-sample as well.
- 10 Add 100 ml 4.5 N HCl, save as Al sample.
- 11
- 12
- 13 **CONDITION CATION COLUMN**

(bottle C1) 100 ml 9N HCl
 (bottle C2) 50 ml 4.5 N HCl
 (bottle C3) 50 ml 1 N HCl
 (bottle C4) 50 ml water
 (bottle C5) 100 ml 0.5 N HCl

WS9_Be Sample Chemistry

This worksheet outlines the steps to prepare the BeO sample

Chemist: ^{GY}

Date: ^{form: mm/dd/yy}

Print this page

- 1 Evaporate Be Sample from column in wiped digestion vessels at 125°C
- 2 Add 2-5 ml 20% perchloric and evaporate at 200°C
- 3 Again, add 2-5 ml 20% perchloric and evaporate at 200°C
- 4 Dissolve sample in 10 ml of 0.5 N HCl (optima grade)
- 5 Transfer to 15 ml centrifuge tube
- 6 Centrifuge and decant into clean centrifuge tube
- 7 Heat centrifuge tubes in water bath at 60°C
- 8 Precipitate Be(OH)₂ using Matheson ultimate grade ammonia gas
Gently bubble NH₃ with clean pipet tip on hose
for ca. 15 bubbles, or ca. 8-12 sec until ptte forms
Optimum pH=9.2; 1N HCl may be added
- 9 Centrifuge 15 min., decant (save and redo 8 if pH of liquid is < 8)
- 10 Wash with water, vortex, centrifuge for 10 min, and decant
- 11 Record mass quartz vials, label, and place them in furnace holder

CNEF ID	1237	1241	1337	1338	1227	1228	1216	1536	105
Sample ID	ME-02-PHD-110	ME-02-DAY-115	ORE-01-McG-05	VAN-01-MYRA-06	MC-02-4	MC-02-5	K02-229-35	Blank	WY-96-001
Mass Qtz Vial	2.426	2.5355	2.4999	2.556	2.5109	2.5713	2.5712	2.4195	2.1400 g
Mass Vial+Spl	2.4269	2.536	2.5003	2.5562	2.5117	2.5725	2.518	2.4204	2.1410 g
Mass Spl	0.0009	0.0005	0.0004	0.0002	0.0008	0.0012	-0.0532	0.0009	1 mg

- 12 Add 1 small drop of water with micropipet, slurry precipitate
- 13 Transfer sample into quartz vial, cover with alumina vial
- 14 Heat in oven at 120°C for 2-3 hours
- 15 Let cool and scrape sample down from walls of quartz tube
- 18 Place in furnace. Convert to BeO in furnace at 850°C for minimum 1 hr
- 19 Determine mass of vial + sample

WS10_AI Sample Chemistry

This worksheet outlines the steps to prepare the Al oxide sample

Chemist: ^{GY}

Date: ^{form: mm/dd/yy}

Print this page

- 1 Evaporate Al Sample from column in wiped teflon vessel at 125°C
- 2 Dissolve sample in 10 ml of 0.5 N HCl (optima grade)
- 3 Transfer to 15 ml centrifuge tube
- 4 Centrifuge and decant into clean centrifuge tube
- 5 Heat centrifuge tubes in water bath at 60°C
- 6 Precipitate Al(OH)₃ using 50% NH₃OH (drops: 25, 5, 5, 3, 2...)

Optimum pH=6.3; 1N HCl may be added

- 7 Centrifuge 15 min., decant (save and redo 6 if pH of liquid is < 8)
- 8 Wash with water, vortex, centrifuge for 10 min, and decant
- 9 Record mass quartz vials, label, and place them in furnace holder

CNEF ID	1237	1241	1337	1338	1227	1228	1216	1536	105
Sample ID	E-02-PHD-	E-02-DAY-	RE-01-McGN-	N-01-MYRA	MC-02-4	MC-02-5	K02-229-35	Blank	WY-96-001
Mass Qtz Vial									2.1400 g
Mass Vial+Spl									2.1410 g
Mass Spl	0	0	0	0	0	0	0	0	1 mg

- 10 Add 1 small drop of water with micropipet, slurry precipitate
- 11 Transfer sample into quartz vial, cover with alumina vial
- 12 Heat in oven at 120°C for 2-3 hours
- 13 Let cool and scrape sample down from walls of quartz tube
- 14 Convert to Al₂O₃ in furnace at 950°C for minimum of 1 hr
- 15 Determine mass of vial + sample

Batch 1									¹⁰ Be/ ⁹ Be Ratio (Corr. for boron)	¹⁰ Be/ ⁹ Be Ratio (Sample bkgd)	¹⁰ Be/ ⁹ Be RATIO (Corr. for bkgd)			
CNEFID	DATE	CAMS #	runs	r_to_rstd	interror	exterror	Truefrac	RATIO	ERROR	RATIO	ERROR	RATIO	ERROR	% Error
1504 Blank	7th Oct 04	BE19691	3	0.0068534	0.0003449	0.001591	0.977	2.131E-14	4.9E-15			2.159E-14	4.9E-15	23%
1236	7th Oct 04	BE19692	2	0.0185938	0.0007018	0.000652	0.991	5.783E-14	2.2E-15	4.1E-15	8.5E-16	5.445E-14	2.3E-15	4%
1237	7th Oct 04	BE19693	2	0.028603	0.0008915	0.000146	0.991	8.896E-14	2.8E-15	4.1E-15	8.5E-16	8.598E-14	2.9E-15	3%
1238	7th Oct 04	BE19694	3	0.0075397	0.0003371	0.00007	0.981008	2.34485E-14	1.048E-15	4.06484E-15	8.5E-16	1.96329E-14	1.352E-15	7%
1239	7th Oct 04	BE19695	3	0.0035709	0.0002304	0.000093	0.97442	1.11055E-14	7.165E-16	4.06484E-15	8.5E-16	7.13121E-15	1.114E-15	16%
1240	7th Oct 04	BE19696	2	0.0103481	0.0005058	2.27E-05	0.984737	3.21826E-14	1.573E-15	4.06484E-15	8.5E-16	2.84794E-14	1.79E-15	6%
1241	7th Oct 04	BE19697	3	0.0127884	0.0004467	0.000111	0.977786	3.97719E-14	1.389E-15	4.06484E-15	8.5E-16	3.61663E-14	1.631E-15	5%
1500 Blank	7th Oct 04	BE19659	2	0.0013024	0.0001779	1.86E-05	0.887	4.050E-15	5.5E-16			4.103E-15	5.5E-16	13%
1501 Blank	7th Oct 04	BE19667	2	0.0015512	0.0001898	3.15E-05	0.958	4.824E-15	5.9E-16			4.886E-15	5.9E-16	12%
1502 Blank	7th Oct 04	BE19675	3	0.0015673	0.0001615	0.000158	0.931	4.874E-15	5.0E-16			4.937E-15	5.0E-16	10%
1503 Blank	7th Oct 04	BE19683	2	0.000963	0.0001431	0.000078	0.907	2.995E-15	4.5E-16			3.033E-15	4.5E-16	15%

Standard used for normalization: LLNL3110
 10/9 ratio for standard = 3.11E-12
 Carrier background for stds = 4.E-14
 Boron correction factor = 0.00008 ± 0.00005 of total events
 KNSTD have a carrier blank of 4E-14

Notes:
 An average of JG-1500, JG-1501, JG-1502 and JG-1503 was used for the blank correction.
 1504 was not included because of its anomalously high value.

Batch 2									¹⁰ Be/ ⁹ Be Ratio (Corr. for boron)		¹⁰ Be/ ⁹ Be Ratio (Sample bkgd)		¹⁰ Be/ ⁹ Be RATIO (Corr. for bkgd)		
CNEFID	DATE	CAMS #	runs	r_to_rstd	interror	exterror	Truefrac	RATIO	ERROR	RATIO	ERROR	RATIO	ERROR	% Error	
1530 Blank	17th Nov 04	BE19896	2	0.0018771	0.0001928	7.91E-05	0.897191	5.83778E-15	5.996E-16			5.91287E-15	5.996E-16	10%	
1229	17th Nov 04	BE19897	2	0.0182264	0.0005937	0.000403	0.985845	5.66841E-14	1.846E-15	5.91287E-15	6E-16	5.14242E-14	1.941E-15	4%	
1230	17th Nov 04	BE19898	3	0.0232002	0.0005511	0.000616	0.989132	7.21526E-14	1.915E-15	5.91287E-15	6E-16	6.70917E-14	2.007E-15	3%	
1231	17th Nov 04	BE19899	4	0.0105532	0.0003203	0.000193	0.991692	3.28205E-14	9.961E-16	5.91287E-15	6E-16	2.72537E-14	1.163E-15	4%	
1232	17th Nov 04	BE19900	2	0.0228961	0.0008646	0.00019	0.9398	7.12069E-14	2.689E-15	5.91287E-15	6E-16	6.61338E-14	2.755E-15	4%	
1233	17th Nov 04	BE19901	2	0.0126691	0.000472	0.000272	0.984825	3.94009E-14	1.468E-15	5.91287E-15	6E-16	3.39188E-14	1.586E-15	5%	

Standard used for normalization: KNSTD3110

10/9 ratio for standard = 3.11E-12

Carrier background for stds = 4.E-14

Boron correction factor = 0.0001 ± 0.00005 of total events

KNSTD have a carrier blank of 4E-14

Note: Sample 1530 was used to make the blank correction

Batch 3									¹⁰ Be/ ⁹ Be Ratio (Corr. for boron)	¹⁰ Be/ ⁹ Be Ratio (Sample bkgd)	¹⁰ Be/ ⁹ Be RATIO (Corr. for bkgd)			
CNEFID	DATE	CAMS #	runs	r_to_rstd	interror	exterror	Truefrac	RATIO	ERROR	RATIO	ERROR	RATIO	ERROR	% Error
1536 Blank	17th Feb 05	BE20396	3	0.0027029	0.0002518	0.000271	0.812267	8.40602E-15	8.416E-16			8.51414E-15	8.416E-16	10%
1237	17th Feb 05	BE20397	2	0.0309553	0.0008463	0.000602	0.974708	9.6271E-14	2.632E-15	7.056E-15	1.1E-15	9.03624E-14	2.834E-15	3%
1241	17th Feb 05	BE20398	2	0.0229274	0.0007981	0.00062	0.970259	7.13042E-14	2.482E-15	7.056E-15	1.1E-15	6.50746E-14	2.696E-15	4%

Standard used for normalization: KNSTD3110
10/9 ratio for standard = 3.11E-12
Carrier background for stds= 4.E-14
Boron correction factor = 0.00006 ± 0.00005 of total events
KNSTD have a carrier blank of 4E-14
Note: Blank correction made using sample 1536

Appendix 3: Snow Depth Calculations

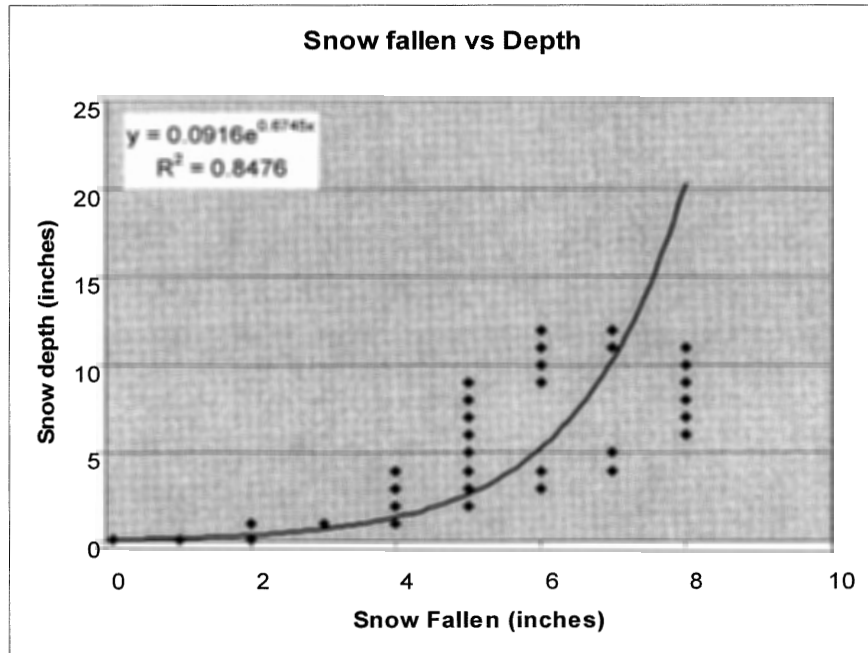


Figure 1. Snow fallen versus Snow depth in Vermont, NH.

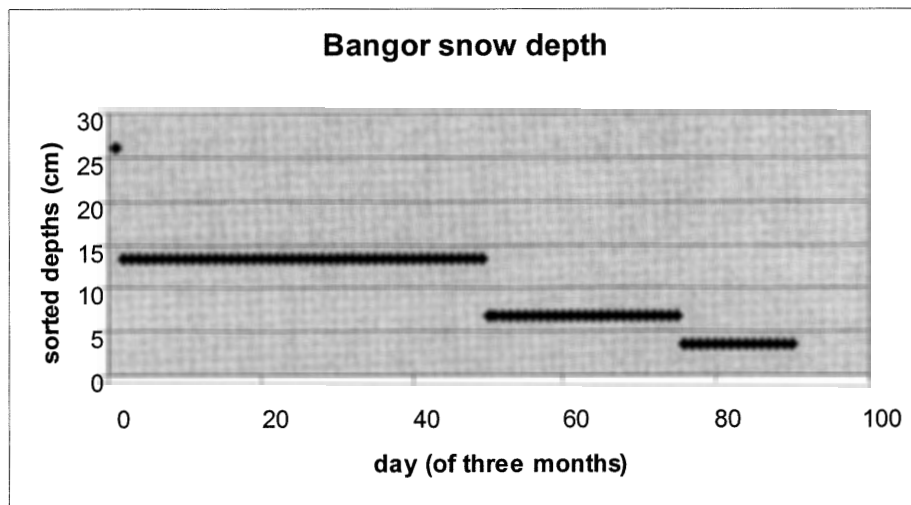


Figure 2. Average Snow depths in Bangor Maine from 1971-2000.